

---

# Rate-Distortion Theoretic Model Compression: Successive Refinement for Pruning

---

**Berivan Isik**

Department of Electrical Engineering  
Stanford University  
berivan.isik@stanford.edu

**Albert No**

Department of Electronic and Electrical Engineering  
Hongik University  
albertno@hongik.ac.kr

**Tsachy Weissman**

Department of Electrical Engineering  
Stanford University  
tsachy@stanford.edu

## Abstract

We study the neural network (NN) compression problem, viewing the tension between the compression ratio and NN performance through the lens of rate-distortion theory. We choose a distortion metric that reflects the effect of NN compression on the model output and then derive the tradeoff between rate (compression ratio) and distortion. In addition to characterizing theoretical limits of NN compression, this formulation shows that *pruning*, implicitly or explicitly, must be a part of a good compression algorithm. This observation bridges a gap between parts of the literature pertaining to NN and data compression, respectively, providing insight into the empirical success of pruning for NN compression. Finally, we propose a novel pruning strategy derived from our information-theoretic formulation and show that it outperforms the relevant baselines on CIFAR-10 and ImageNet datasets.

## 1 Introduction

The recent success of NNs in various machine learning applications has come with their over-parameterization [16, 57]. Deployment of such over-parameterized models on edge devices is challenging as these devices have limited storage, computation, and power resources. Motivated by this, there has been significant interest in NN compression by the research community [7, 11]. The most established NN compression techniques can be broadly grouped into five categories: quantization [3, 12, 45, 48, 49, 60, 91, 97, 104, 105] and coding [38, 77, 100, 108] of NN parameters, pruning [6, 8, 19, 20, 26, 35, 54, 61, 62, 64, 65, 66, 72, 78, 80, 82, 85, 89, 90, 98, 102, 103, 106, 107], Bayesian compression [15, 23, 67, 68, 71, 101], distillation [32, 40, 81, 96], and low-rank matrix factorization [43, 44, 46, 83]. The fact that these techniques have achieved compressing NN models without a significant performance loss brings a theoretical question: *what is the highest achievable compression ratio given a target performance for the compressed model?*

A similar question arises in the classical data compression problem as well [84]. Shannon introduced the mathematical formulation of the data compression problem, where the goal is to describe a source sequence with the minimum number of bits [87]. In an information-theoretic sense, entropy is the limit of how much a source sequence can be losslessly compressed. However, *in practice*, there are many sources such as image, video, and audio, where lossless compression cannot achieve a high enough compression rate. In such cases, we need to compress the source sequence in a *lossy* manner allowing some *distortion* between the source and reconstruction. This is where rate-distortion theory

comes into the picture. For lossy compression, rate-distortion theory gives the limit of how much a source sequence can be compressed without exceeding a target distortion level [5].

In this work, we connect these two lines of research and study the theoretical limits of lossy NN compression via rate-distortion theory. In particular, we consider a classical lossy compression problem to compress NN weights while minimizing the perturbation in the NN output space. We first (1) define a distortion metric that upper bounds the output perturbation due to compression, then (2) find a probability distribution that fits NN parameters, and finally (3) derive the rate-distortion function for the chosen distortion metric and distribution. This function describes the theoretical tradeoff between rate (compression ratio) and NN output perturbation, thus providing insight into how compressible NN models are. Furthermore, our findings indicate that the compressed model that reaches the optimal achievable compression ratio must be sparse. This suggests that a good NN compression algorithm must, implicitly or explicitly, involve a pruning step, complimenting the empirical success of pruning strategies [27]. Therefore, we provide theoretical support for pruning as a rate-distortion theoretic compression scheme that maintains the model output.

Inspired by this observation, we propose a practical lossy compression algorithm for NN models. The reconstruction of our algorithm is a sparse model, which naturally induces a novel pruning strategy. Our algorithm is based on *successive refinability* – a property that often helps to reduce the complexity of lossy compression algorithms [21]. Our strategy differs from previous score-based pruning methods as it relies solely on an information-theoretic approach to a data compression problem with additional practical benefits that we cover in Section 6. We also prove that the proposed algorithm is sound from a rate-distortion theoretic perspective. We demonstrate the efficacy of our pruning strategy on CIFAR-10 and ImageNet datasets. Lastly, we show that our strategy provides a tool for compressing NN gradients as well, an important objective in communication-efficient federated learning (FL) settings [50]. The contributions of our paper can be summarized as:

- We take a step in bridging the gap between NN compression and data compression.
- We present the rate-distortion theoretical limit of achievable NN compression given a target distortion level and show that pruning is an essential part of a good compression algorithm.
- We propose a novel pruning strategy derived from our findings, which outperforms relevant baselines in the literature.

## 2 Related Work

This section is devoted to prior work on NN compression that has the same flavor as ours, in particular, we touch on (a) data compression approaches to NN compression and (b) pruning. We cover related works in classical data compression as we go through the methodology in Sections 3, 4, and 5.

**Data Compression Approaches to NN Compression.** To date, several works have proposed to minimize the bit-rate (compressed size) of NNs with quantization techniques [45, 91, 97]. Some recent work has shown promising results to go beyond quantization using tools from data compression. For instance, Havasi et al. [38] and Oktay et al. [77] have trained a model to jointly optimize compression and performance of the model using tools from minimum description length principle [33] and a recently advanced image compression framework [2], respectively. While we share the same goal with these papers, our focus is on compressing any NN model *post-training*. With this distinction, our work is most related to [30], where the authors have put the first attempt to approach NN compression from a rate-distortion theoretic perspective. While they have shown achievability results on one-layer networks, their results do not generalize to deeper networks without first-order Taylor approximations. Moreover, their formulation relies on the assumption that NN weights follow a Gaussian distribution, which currently lacks empirical evidence. On the other hand, we show achievable compression ratios generalized to multi-layer networks without making linear approximations and provide strong empirical evidence for our choice of *Laplacian* distribution for NN weights.

**Pruning.** Starting from early works of [9, 14, 37], overparameterized nature of NNs has motivated researchers to explore ways to find and remove redundant parameters. The idea of iterative magnitude pruning was shown to be remarkably successful in deep NNs first by Han et al. [36], and since then, NN pruning research has accelerated. To improve upon the iterative magnitude pruning scheme of [36], researchers have looked for more clever ways to adjust the pruning ratios across layers. For

instance, [109] have suggested pruning the parameters uniformly across layers. Gale et al. [28], on the other hand, have shown better results when the first convolutional layer is excluded from the pruning and the last fully-connected layer is not pruned more than 80%. Layerwise pruning ratio has also been investigated for NNs pruned at initialization since the explosion of the Lottery Ticket Hypothesis [24, 25, 73]. Evci et al. [22] have shown promising results on NNs pruned at initialization where the pruning ratio across layers is adjusted by Erdős-Rényi kernel method, as introduced in [70]. More recently, Lee et al. [58] have proposed adjusting the pruning threshold for each layer based on the norm of the weights at that layer. We follow a similar methodology in [58] to normalize the parameters prior to applying our *novel* pruning algorithm. Unlike other pruning strategies, our algorithm outputs a pruned (sparse) model, without explicitly performing a score-based pruning step. Instead, we develop the algorithm from a theoretical formulation of the NN compression problem, where our reconstruction goes from the coarsest (sparsest) to the finest representation of the model. Parallel to our work, a recent study has proposed a heuristic bottom-up approach as opposed to the common top-down pruning approach and provided promising empirical results [10]. To the best of our knowledge, our work is the first to provide a rate-distortion theoretic foundation for pruning.

### 3 Preliminaries

In this section, we present the problem setup and briefly introduce the rate-distortion theory and the successive refinement concept.

**Problem Statement:** We study a NN compression problem where the network  $\mathbf{y} = f(\mathbf{x}; \mathbf{w})$  characterizes a prediction from the input space  $\mathcal{X}$  to the output space  $\mathcal{Y}$ , parameterized by weights  $\mathbf{w}$ . Our goal is to minimize the difference between  $\mathbf{y} = f(\mathbf{x}; \mathbf{w})$  and  $\hat{\mathbf{y}} = f(\mathbf{x}; \hat{\mathbf{w}})$ , where  $\hat{\mathbf{w}}$  is a compressed version of the trained parameters  $\mathbf{w}$ . In Section 4.1, we define an appropriate distortion function  $d(\mathbf{w}, \hat{\mathbf{w}})$  that reflects the perturbation in the output space  $\|f(\mathbf{x}; \mathbf{w}) - f(\mathbf{x}; \hat{\mathbf{w}})\|_1$ . This is a lossy compression problem where the distortion is a measure of the distance between the original model and the compressed model, and the rate is the number of bits required to represent one weight. In information-theoretic term, rate distortion theory characterizes the minimum achievable rate given the target distortion.

**Notation:** Throughout the paper,  $\mathbf{w} \in \mathbb{R}^n$  is the weights of a trained model. Logarithms are natural logarithms. Rate is defined as nats (the unit of information obtained from natural logarithm) per symbol (weight in our case). We use lower case  $u$  to denote the realization of a scalar random variable  $U$  and  $\mathbf{u} = u^n = (u_1, \dots, u_n)$  to denote the realization of a random vector  $\mathbf{U} = U^n = (U_1, \dots, U_n)$ . We use the term “perturbation” for the change in the model output due to compression, whereas “distortion”  $d(\mathbf{w}, \hat{\mathbf{w}})$  refers to the change in the *parameter* space. Lastly,  $d(u^n, \hat{u}^n) = \frac{1}{n} \sum_{i=1}^n d(u_i, \hat{u}_i)$  is the regular extension of the distortion function for an  $n$  dimensional vector.

**Rate-Distortion Theory:** Let  $U_1, \dots, U_n \in \mathcal{U}$  be a source sequence generated by i.i.d.  $\sim p(u)$  where  $p(u)$  is a probability density function and  $\mathcal{U} = \mathbb{R}$ . The encoder  $f_e : \mathcal{U}^n \rightarrow \{0, 1\}^{nR}$  describes this sequence in  $nR$  bits, where this binary representation is called a “message”  $m$ . The decoder  $f_d : \{0, 1\}^{nR} \rightarrow \hat{\mathcal{U}}^n$  reconstructs an estimate  $\hat{\mathbf{u}} = \hat{u}^n \in \hat{\mathcal{U}}^n$  based on  $m \in \{0, 1\}^{nR}$  where  $\hat{\mathcal{U}} = \mathbb{R}$  as well. The number of bits per source symbol ( $\frac{nR}{n} = R$  in this case) and the “distance”  $d(\mathbf{u}, \hat{\mathbf{u}}) = d(u^n, \hat{u}^n) = \frac{1}{n} \sum_{i=1}^n d(u_i, \hat{u}_i)$  between  $\mathbf{u}$  and  $\hat{\mathbf{u}}$  are named as rate and distortion, respectively. Ideally, we would like to keep both rate and distortion low, but there is a tradeoff between these two quantities, which is characterized by the rate-distortion function [87, 5, 13] as:

$$R(D) = \min_{p(\hat{u}|u) : \mathbb{E}[d(u, \hat{u})] \leq D} I(U; \hat{U}) \quad (1)$$

where  $I(U; \hat{U})$  is the mutual information between  $U$  and  $\hat{U}$ , and  $d(\cdot, \cdot)$  is a predefined distortion metric, e.g.  $\ell_2$  distance. The rate-distortion function  $R(D)$  in Eq. 1 is the minimum achievable rate at distortion  $D$ , and the conditional distribution  $p(\hat{u}|u)$  that achieves  $I(U; \hat{U}) = R(D)$  explains how an optimal encoder-decoder pair should operate for the source  $p(u)$ . We can also define the inverse, namely the distortion-rate function  $D(R)$ , which is the minimum achievable distortion at rate  $R$ . Clearly, source distribution has a critical role in the solution of the rate distortion problem. We discuss possible assumptions for the distribution of NN weights in Section 4.2.

**Successive Refinement:** In the successive refinement problem, the encoder wants to describe the source to two decoders, where each decoder has its own target distortion,  $D_1$  and  $D_2$ . Instead of

having separate encoding schemes for each decoder, the successive refinement encoder encodes a message  $m_1$  for Decoder 1 (with higher target distortion,  $D_1$ ), and encodes an extra message  $m_2$  where the second decoder gets both  $m_1$  and  $m_2$ . Receiving both  $m_1$  and  $m_2$ , Decoder 2 reconstructs  $\hat{\mathbf{U}}_2$  with distortion  $D_2$ . Since the message  $m_1$  is re-used, the performance of successive refinement encoder is sub-optimal in general. However, in some cases, the successive refinement encoder achieves the optimum rate-distortion tradeoff as if dedicated encoders were used separately. In such a case, we call the source (distribution) and the distortion pair successively refinable [21, 52]. In Section 5.1, we discuss how to achieve low complexity via successive refinement.

## 4 Rate-Distortion Theory for Neural Network Parameters

In this section, we first derive the distortion metric to be used in the rate-distortion function, then we estimate the source distribution (probability density of NN weights), and finally, we present the rate-distortion function associated with the chosen distortion metric and the source distribution.

### 4.1 Distortion Metric

Our objective is to minimize the difference between the output of the original NN model and the compressed model. Formally, we would like to keep the output perturbation  $\|f(\mathbf{x}; \mathbf{w}) - f(\mathbf{x}; \hat{\mathbf{w}})\|_1$  small. Since the effect of a weight distortion on the output space  $f(\mathbf{x}; \mathbf{w})$  is intractable for deep NNs, we seek to find a distortion function on parameter space that upper bounds  $\|f(\mathbf{x}; \mathbf{w}) - f(\mathbf{x}; \hat{\mathbf{w}})\|_1$ .

Prior work has derived an upper bound for  $\ell_2$  norm of output perturbation involving Frobenius norm of the difference between  $\mathbf{w}$  and  $\hat{\mathbf{w}}$  when only the single layer is compressed [58]. More precisely, consider a NN model with  $d$  layers. Let  $\mathbf{w}$  be the weights of the original trained model and  $\hat{\mathbf{w}}$  be a compressed version of  $\mathbf{w}$  where  $\hat{\mathbf{w}}$  is the same with  $\mathbf{w}$  except in the  $l$ -th layer. In such a case, i.e., when only a single layer is compressed, the output perturbation is bounded by

$$\sup_{\|\mathbf{x}\|_2 \leq 1} \|f(\mathbf{x}; \mathbf{w}) - f(\mathbf{x}; \hat{\mathbf{w}})\|_2 \leq \frac{\|\mathbf{w}^{(l)} - \hat{\mathbf{w}}^{(l)}\|_F}{\|\mathbf{w}^{(l)}\|_F} \cdot \left( \prod_{k=1}^d \|\mathbf{w}^{(k)}\|_F \right) \quad (2)$$

where  $\mathbf{w}^{(l)}$  indicates the weights of the  $l$ -th layer. Inspired by Eq. 2, Lee et al. [58] have introduced Layer-Adaptive Magnitude-based Pruning (LAMP) score  $(\mathbf{w}_i^{(l)})^2 / (\sum_j (\mathbf{w}_j^{(l)})^2)$  to measure the importance of the weight  $\mathbf{w}_i^{(l)}$  for pruning. Notice that Eq. 2 holds only when a single layer is pruned.

In this work, we follow a similar strategy to relate the “ $\ell_1$  norm of perturbation on the output space” to “ $\ell_1$  norm of the weight difference due to compression”, but not limited to single-layer compression.

**Theorem 1.** Suppose  $f(\cdot; \mathbf{w})$  is a fully-connected NN model with  $d$  layers and 1-Lipschitz activations, e.g., ReLU. Let  $\hat{\mathbf{w}}$  be the reconstructed weight (after compression) where all layers are subject to compression. Then, we have the following bound on the output perturbation:

$$\sup_{\|\mathbf{x}\|_1 \leq 1} \|f(\mathbf{x}, \mathbf{w}) - f(\mathbf{x}, \hat{\mathbf{w}})\|_1 \leq \left( \sum_{l=1}^d \frac{\|\mathbf{w}^{(l)} - \hat{\mathbf{w}}^{(l)}\|_1}{\|\mathbf{w}^{(l)}\|_1} \right) \left( \prod_{k=1}^d \|\mathbf{w}^{(k)}\|_1 \right) \quad (3)$$

i.e., the output perturbation is bounded by the  $\ell_1$  distortion of normalized weights.

The matrix norm  $\|\cdot\|_1$  is an induced norm by  $\ell_1$  vector norm. The proof is given in Appendix A. In Section 5.2 (Remark 2), we show that the proposed compression algorithm satisfies the additional assumption  $\|\mathbf{w}^{(l)}\|_1 \geq \|\hat{\mathbf{w}}^{(l)}\|_1$  for all  $1 \leq l \leq d$ . Since the last term in Eq. 3,  $\left( \prod_{k=1}^d \|\mathbf{w}^{(k)}\|_1 \right)$ , is independent of the compression, we do not include this term in our weight distortion function. One distortion function that naturally arises from Theorem 1 is  $d(\mathbf{w}, \hat{\mathbf{w}}) = \sum_{l=1}^d \frac{\|\mathbf{w}^{(l)} - \hat{\mathbf{w}}^{(l)}\|_1}{\|\mathbf{w}^{(l)}\|_1}$ . By changing the notation slightly, we would like to minimize the following distortion function

$$d(\mathbf{u}, \hat{\mathbf{u}}) = \frac{1}{n} \sum_{i=1}^n |u_i - \hat{u}_i| \quad (4)$$

where  $\mathbf{u}$  is the normalized weights arisen from the normalization in Eq. 3, i.e.,  $\mathbf{u}^{(l)} = \frac{\mathbf{w}^{(l)}}{\|\mathbf{w}^{(l)}\|_1}$  for  $l = 1, \dots, d$ . In the next section, we derive the rate-distortion function with the distortion metric in Eq. 4, which approximates the perturbation ( $\ell_1$  loss) on the output space due to compression.

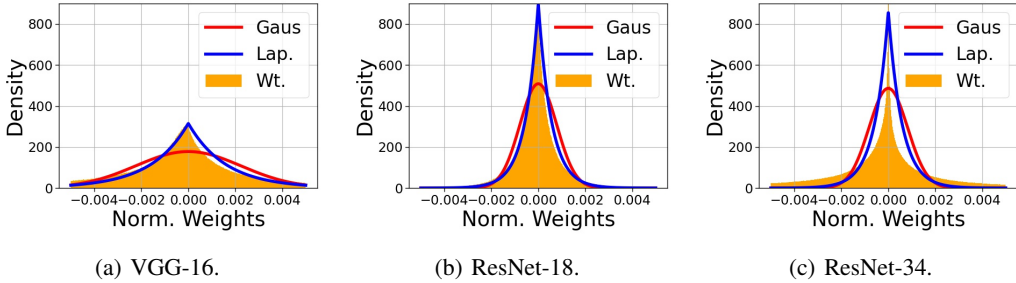


Figure 1: Density of normalized weights. (a) VGG-16, (b) ResNet-18, and (c) ResNet-34. Gaus: Gaussian, Lap.: Laplacian, Wt.: Normalized NN weights.

## 4.2 Rate-Distortion Function for Neural Network Parameters

Since we define our distortion function as the  $\ell_1$  distortion between  $\mathbf{u}$  and  $\hat{\mathbf{u}}$  as in Eq. 4, where  $\mathbf{u}$  is the normalized NN weights, we can formulate the compression problem as a lossy compression of the normalized NN weights. Before deriving the rate-distortion function, we need a source distribution that fits the normalized weights  $\mathbf{u}$ . Figure 1 shows that Laplacian distribution is a good fit for trained NN weights after normalization (we show that it is a good fit without the normalization as well in Appendix B) as opposed to the common Gaussian assumption in the prior work [30].

Now that we have a distortion metric and a source distribution, suitable for NN compression problem, we can finally derive the rate-distortion function. We consider i.i.d. Laplacian source sequence  $u_1, \dots, u_n$  distributed according to  $f_L(u; \lambda) = \frac{\lambda}{2} e^{-\lambda|u|}$  with zero-mean and scale factor of  $\lambda$ , reconstructed sequence  $v_1, \dots, v_n$ , and  $\ell_1$  distortion given in Eq. 4 with  $\hat{\mathbf{u}} = \mathbf{v}$ . The rate-distortion function, which is the minimum achievable rate given the target distortion  $D$  follows by:

**Lemma 1** ([5]). *The rate-distortion function for a Laplacian source with  $\ell_1$  distortion is given by*

$$R(D) = \begin{cases} -\log(\lambda D), & 0 \leq D \leq \frac{1}{\lambda} \\ 0, & D > \frac{1}{\lambda} \end{cases} \quad (5)$$

with the following optimal conditional probability distribution that achieves the minimum rate:  $f_{\mathbf{U}|\mathbf{V}}(u|v) = \frac{1}{2D} e^{-|u-v|/D}$ . Moreover, the marginal distribution of  $\mathbf{V}$  for the optimal reconstruction is  $f_{\mathbf{V}}(v) = \lambda^2 D^2 \cdot \delta(v) + (1 - \lambda^2 D^2) \cdot \frac{\lambda}{2} e^{-\lambda|v|}$ , where  $\delta(v)$  is a Dirac measure at 0.

The proof of Lemma 1 is given in Appendix C. The rate-distortion function in Eq. 5 describes the tradeoff between NN compression ratio and weight distortion  $D$  – which upper bounds the *output* perturbation. Lemma 1 further indicates that:

- (1) The rate-distortion theoretic optimal encoder-decoder pair makes the reconstruction sparse as the marginal distribution in Lemma 1 is a sparse Laplacian distribution where  $\lambda^2 D^2$  fraction of the elements are 0. More concretely, the reconstructed NN model must be sparse to satisfy the conditions for the optimal compression scheme. Therefore, unless a compression scheme involves an implicit or explicit pruning step (to make the reconstruction sparse), the reconstruction does not follow the marginal distribution in Lemma 1. This would make the compression scheme sub-optimal since the mutual information between the source  $\mathbf{U}$  and the reconstruction  $\hat{\mathbf{U}}$  would be strictly larger than the rate-distortion function.
- (2) Once  $\mathbf{V}$  is reconstructed at the decoder, the error term on the encoder side,  $\mathbf{U} - \mathbf{V}$ , follows a Laplacian distribution with parameter  $1/D$  (see conditional distribution in Lemma 1). This allows for a practical coding scheme with low complexity based on successive refinement. That is, we can iteratively<sup>1</sup> describe NN weights with reasonable complexity.

In Theorem 1, we add another constraint that the norm of the reconstructed weights at each layer is smaller than the norm of the original weights at the same layer ( $\|\mathbf{w}^{(l)}\|_1 \geq \|\hat{\mathbf{w}}^{(l)}\|_1$ ). This is mainly because (1) sign change in the NN weights can significantly affect the NN output, hence sign bits

<sup>1</sup>The term “iterative” in our proposed algorithm is different from the “iterative” magnitude pruning concept.

must be protected to maintain the performance [47]; and (2) this inequality ( $\|\mathbf{w}^{(l)}\|_1 \geq \|\hat{\mathbf{w}}^{(l)}\|_1$ ) is necessary to apply the iterative compression algorithm based on successive refinement (to be discussed in Section 5).

In the next section, we develop a NN compression algorithm merging (i) our theoretical findings in Lemma 1 for *optimality* and (ii) successive refinement property for *practicality*.

## 5 Successive Refinement for Pruning (SuRP)

Rate-distortion theory, although, gives the limit of lossy compression and suggests that pruning must be a part of a good compression algorithm, does not explicitly give the optimal compression algorithm. In *theory*, a compression algorithm could be designed by letting the encoder pick the closest codeword from a random codebook generated according to the marginal distribution of  $\mathbf{V}$  in Lemma 1, as suggested by Shannon [87]. However, such a compressor would not be practical due to the size of the randomly generated codebook  $|\mathcal{C}| = 2^{nR(D)}$  (exponential in  $n$  – number of weights in our case). While designing practical compression algorithms without sacrificing the optimality is a fundamental dilemma in data compression, recent studies have shown that it is possible to design theoretically optimal schemes with low complexity for certain source distributions. In particular, for a successively refinable source, an optimal compression algorithm can also be practical [76]. We exploit this idea for the Laplacian source and develop a practical iterative compression algorithm that is rate-distortion theoretically optimal. We call it Successive Refinement for Pruning (SuRP) since it also outputs a sparse model, which can be viewed as a pruned model (although we do not explicitly prune the model). We first present the successive refinement scheme for Laplacian source that shows the core idea to achieve lower complexity, but still impractical. We then push further to provide the practical algorithm and prove the optimality in a rate-distortion theoretic sense.

### 5.1 Successive Refinement with Randomly Generated Codebooks

Instead of a successive refinement scheme with two decoders as described in Section 3, we consider the successive refinement problem with  $L$  decoders. Let  $\lambda = \lambda_1 < \dots < \lambda_L$  where  $D_t = 1/\lambda_{t+1}$  is a target distortion at the  $t$ -th decoder. This is because the error term at iteration  $t$  has a Laplacian distribution with parameter  $\lambda_{t+1} = 1/D_t$  in an optimal compression scheme (see Lemma 1). We begin by setting  $\mathbf{U}^{(1)} = u^n$ . At  $t$ -th iteration, the encoder finds  $\mathbf{V}^{(t)}$  that minimizes the distance between  $d(\mathbf{U}^{(t)}, \mathbf{V}^{(t)})$  from a codebook  $\mathcal{C}^{(t)}$ , then computes  $\mathbf{U}^{(t+1)} = \mathbf{U}^{(t)} - \mathbf{V}^{(t)}$ . More precisely, the  $t$ -th codebook consists of  $2^{nR/L}$  codewords generated by the marginal distribution in Lemma 1:

$$f_{\mathbf{V}^{(t)}}(v) = \frac{\lambda_t^2}{\lambda_{t+1}^2} \cdot \delta(v) + \left(1 - \frac{\lambda_t^2}{\lambda_{t+1}^2}\right) \cdot \frac{\lambda_t}{2} e^{-\lambda_t|v|} \quad (6)$$

Since  $\mathbf{U}^{(t+1)}$  is also an i.i.d. Laplacian random sequence with parameter  $\lambda_{t+1} = 1/D_t$  from the conditional probability in Lemma 1, the encoder can keep applying the same steps for Laplacian sources at each iteration. In summary, for  $1 \leq t \leq L-1$ , the information-theoretic successive refinement encoder performs the following steps iteratively: (1) find  $\mathbf{V}^{(t)} \in \mathcal{C}^{(t)}$  that minimizes  $d(\mathbf{U}^{(t)}, \mathbf{V}^{(t)})$ ; and (2) update  $\mathbf{U}$  as  $\mathbf{U}^{(t+1)} = \mathbf{U}^{(t)} - \mathbf{V}^{(t)}$ . The decoder, on the other hand, reconstructs  $\hat{\mathbf{U}}^{(t)} = \sum_{\tau=1}^t \mathbf{V}^{(\tau)}$  at iteration  $t$ . This scheme has a complexity of  $L \cdot 2^{nR/L}$  (the total size of the codebooks in  $L$  iterations), which is lower than the naive random coding strategy ( $2^{nR}$  at once). At the same time, it still achieves the rate-distortion limit, i.e., does not sacrifice the optimality, thanks to successive refinability of Laplacian source. However, the complexity is still exponential in  $n$ , which is impractical. We fix this in the next section.

### 5.2 SuRP Algorithm

We saw in Section 5.1 that the information-theoretic approach is rate-distortion theoretic optimal with lower complexity due to successive refinability, but still impractical with the exponential size of codebooks. In this section, we develop a new algorithm SuRP, that enjoys both practicality and optimality. Concretely, SuRP does not require a random codebook or a search for the nearest codeword  $\mathbf{V}^{(t)}$  from  $\mathbf{U}^{(t)}$  at each iteration, yet still rate-distortion theoretic optimal. With the same initialization  $\mathbf{U}^{(1)} = u^n$  and  $\lambda_1 = \lambda$ , new iterative coding scheme for  $1 \leq t \leq L-1$  is as follows:

1. Find index  $i$  and  $j$  such that  $\mathbf{U}_i^{(t)} \geq \frac{1}{\lambda_t} \log \frac{n}{2\beta}$  and  $\mathbf{U}_j^{(t)} \leq -\frac{1}{\lambda_t} \log \frac{n}{2\beta}$ . If there are more than one such indices, pick an index  $i$  (or  $j$ ) randomly. Encode  $(i, j)$  as  $m_t$ .
2. Let  $\mathbf{V}^{(t)}$  be an  $n$ -dimensional all-zero vector except  $\mathbf{V}_i^{(t)} = \frac{1}{\lambda_t} \log \frac{n}{2\beta}$  and  $\mathbf{V}_j^{(t)} = -\frac{1}{\lambda_t} \log \frac{n}{2\beta}$ .
3. Let  $\mathbf{U}^{(t+1)} = \mathbf{U}^{(t)} - \mathbf{V}^{(t)}$ .
4. Set  $\lambda_{t+1} = \frac{n}{n-2\log \frac{n}{2\beta}} \cdot \lambda_t$ .

Here,  $\beta > 1$  is a tunable parameter. Similar to the algorithm in Section 5.1, the reconstruction at  $t$ -th iteration would be  $\hat{\mathbf{U}}^{(t)} = \sum_{\tau=1}^t \mathbf{V}^{(\tau)}$ . We give the pseudocode for SuRP in Appendix D.

This coding scheme is equivalent to the original scheme in Section 5.1, where  $\frac{\lambda_t}{\lambda_{t+1}} = \frac{n-2\log \frac{n}{2\beta}}{n}$  for  $1 \leq t \leq L-1$  except the fact that the encoder does not do a search over a randomly generated codebook with exponential size, i.e., SuRP is practical. However, there is still an *implicit* codebook  $\mathcal{C}^{(t)}$  at every iteration  $t$ , which consists of  $n$ -dimensional all-zero vectors except for two nonzero elements of values  $\pm \frac{1}{\lambda_{t-1}} \log \frac{n}{2\beta}$ . The size of this codebook is  $n(n-1)$  (not exponential anymore). Since these *implicit* codebooks are not directly generated from the optimal marginal distribution in Lemma 1, it is not obvious that SuRP is rate-distortion theoretic optimal. However, we prove in Section 5.3 that it is rate-distortion theoretic optimal under certain criteria. We highlight that our scheme can be viewed as a bottom-up approach, in that sparsity in the reconstructed weights starts from 100% at the first iteration and it decreases as the decoder receives new indices from the encoder (see Figure 2-right). Similarly, from the same figure, accuracy increases through the iterations.

As a practical issue, when there is no index  $i$  or  $j$  such that  $\mathbf{U}_i^{(t)} \geq \frac{1}{\lambda_{t-1}} \log \frac{n}{2\beta}$  or  $\mathbf{U}_j^{(t)} \leq -\frac{1}{\lambda_{t-1}} \log \frac{n}{2\beta}$ , the encoder re-estimates  $\lambda$  and sends a refreshed value to the decoder. However, this is a rare situation in our experiments (20 refreshments in 20M iterations) and hence has a negligible effect on the overall optimality. In fact, we control the probability of this undesired situation (when there is no index to send) with the tunable parameter  $\beta$ . More precisely, the probability that all Laplacian random variables are smaller than  $\frac{1}{\lambda} \log \frac{n}{2\beta}$  in magnitude (i.e., no index  $i$  or  $j$  found) is

$$\Pr \left[ \max X_i < \frac{1}{\lambda} \log \frac{n}{2\beta} \text{ or } \min X_i > -\frac{1}{\lambda} \log \frac{n}{2\beta} \right] \quad (7)$$

$$\leq \Pr \left[ \max X_i < \frac{1}{\lambda} \log \frac{n}{2\beta} \right] + \Pr \left[ \min X_i > -\frac{1}{\lambda} \log \frac{n}{2\beta} \right] = 2 \left( 1 - \frac{1}{2} \frac{2\beta}{n} \right)^n \approx 2e^{-\beta}. \quad (8)$$

We set  $\beta = \log n$  to bound the probability in Eq. 8 by  $\frac{2}{n}$ , which converges to zero as  $n$  increases.

**Remark 1.** *From the extreme value theory, it is known that the maximum of  $n$  Laplacian random variables concentrates near  $\frac{1}{\lambda} \log \frac{n}{2}$ , which is the case of  $\beta = 1$ . Thus, one iteration of SuRP can be viewed as finding a near-maximum (and minimum) element. From this perspective, magnitude pruning can be viewed as a special case of SuRP.*

**Remark 2.** *SuRP guarantees  $\|\mathbf{U}^{(t)}\|_1 \geq \|\mathbf{V}^{(t)}\|_1$  for all  $t$ . This implies that the magnitude of weights in  $\mathbf{w}$  is always larger than the magnitude of weights in  $\hat{\mathbf{w}}$ . From Theorem 1, we can say that the  $\ell_1$  weight distortion of SuRP algorithm is an upper bound to the NN model's output perturbation.*

### 5.3 Zero-Rate Optimality of SuRP

In this section, we prove that SuRP is a zero-rate optimal compression algorithm. Given that SuRP uses an *implicit* codebook of size  $n(n-1)$  at each iteration, the rate is found as  $R_n = \frac{\log n(n-1)}{n}$ . We note that  $R_n$  gets arbitrarily close to zero as  $n$  increases. Moreover, the decrement in the distortion at each iteration is given as  $D_n = \frac{2}{n\lambda} \log \frac{n}{2\beta_n}$ , where  $\beta_n = \beta$  as before. We start with the definition of *zero-rate optimality*, which states that a sub-linear number of bits (in our case  $\log n(n-1)$  nats) is being used optimally in the rate-distortion theoretic sense.

**Definition 1** (Zero-rate optimality). *A scheme with rate  $R_n$ , distortion decrement  $D_n$ , and distortion-rate function  $D(\cdot)$ , is zero-rate optimal if  $\lim_{n \rightarrow \infty} R_n = 0$  and  $\lim_{n \rightarrow \infty} \frac{D_n}{R_n} = D'(0)$ .*

This implies that a zero-rate optimal scheme achieves the “slope” of the distortion-rate function at zero rate  $R = 0$ . In the case of Laplacian source, this slope is  $D'(0) = -\frac{1}{\lambda}$  since the distortion-rate function is  $D(R) = \frac{1}{\lambda}e^{-R}$ , which can be derived from the rate-distortion function in Lemma 1. Finally, the following theorem states that a single iteration of SuRP is zero-rate optimal.

**Theorem 2.** *An iteration of SuRP is zero-rate optimal if  $\lim_{n \rightarrow \infty} \frac{\log 2\beta_n}{\log n(n-1)} = 0$  holds.*

*Proof.* In an iteration of SuRP, where  $R_n = \frac{\log n(n-1)}{n}$  and  $D_n = \frac{2}{n\lambda} \log \frac{n}{2\beta_n}$ , we have

$$\frac{D_n}{R_n} = -\frac{\frac{2}{\lambda} \log \frac{n}{2\beta_n}}{\log n(n-1)} = -\frac{1}{\lambda} \frac{\log n^2}{\log n(n-1)} + \frac{1}{\lambda} \frac{2 \log 2\beta_n}{\log n(n-1)}. \quad (9)$$

If  $\lim_{n \rightarrow \infty} \frac{\log 2\beta_n}{\log n(n-1)} = 0$ , it is clear that  $\frac{D_n}{R_n}$  converges to  $D'(0) = -\frac{1}{\lambda}$  as  $n$  increases. Therefore, SuRP is zero-rate optimal under the condition that  $\lim_{n \rightarrow \infty} \frac{\log 2\beta_n}{\log n(n-1)} = 0$ .  $\square$

In Section 5.2, we choose  $\beta_n = \log n$  to keep the probability in Eq. 8 small. With this choice of  $\beta_n$ ,  $\lim_{n \rightarrow \infty} \frac{\log 2\beta_n}{\log n(n-1)} = 0$  holds. Therefore, from Theorem 2, our implementation of SuRP is indeed zero-rate optimal.

**Remark 3.** *In pure information-theoretic compression setting (main concern is not NN compression), similar zero-rate optimal schemes were proposed [75, 93] for Gaussian source under mean squared error, which is also successively refinable. They iteratively applied zero-rate optimal schemes and further achieved the rate-distortion limit using a special property of Gaussian random variables.*

## 6 Experiments

In this section, we empirically investigate (1) the performance of SuRP compared to other recent pruning strategies in terms of accuracy-sparsity tradeoff and (2) improvements in the communication efficiency of federated learning when gradients are compressed with SuRP. We emphasize that the main contribution of our paper is to bridge the gap between data compression and NN compression through a rate-distortion theoretic analysis of NN compression problem. SuRP is designed solely to show that an algorithm derived with an information-theoretic approach indeed outputs a pruned model, as suggested by the rate-distortion theory. This also provides theoretical support for the recent success of pruning strategies.

For ease of implementation, instead of reconstructing two weights larger than  $\frac{1}{\lambda} \log \frac{n}{2\beta}$  in magnitude at each iteration, we reconstruct one weight larger than  $\frac{1}{\lambda} \log \frac{n}{\beta}$ . This is equivalent to the algorithm described in Section 5, and the zero-rate optimality still holds (see Appendix D for details). We present experimental results averaged over 3-5 runs (see Appendix I for complete results).

We consider three image datasets: CIFAR-10 [53] and ImageNet [17] for NN compression and MNIST [56] for federated learning experiments. For MNIST, we use LeNet-5-Caffe. For CIFAR-10, we use two architectures: ResNet-20 [39] and VGG-16 [88]. For ImageNet, we use ResNet-50 [39, 79]. We give additional details on model architectures and hyperparameters in Appendix H.

**NN Compression/Pruning:** In Table 1 and Figure 2-left, we compare our scheme with the recent pruning papers. We apply iterative pruning, meaning that we apply SuRP in repeating cycles (see Appendix I for details). As baselines, we consider Global [73], Uniform [109], and Adaptive [27] pruning techniques and LAMP [58]. Additionally, we include comparisons to recent works on weight rewinding and dynamic sparsity, in particular SNIP [59], DSR [74], SNFS [18], and RiGL [22].

We present the performance of pruned ResNet-50 on ImageNet in Figure 2-left, and VGG-16 and ResNet-20 architectures on CIFAR-10 in Table 1. As can be seen from Table 1, SuRP outperforms prior work in all sparsity levels. From Figure 2-left, SuRP and Adaptive pruning [28] perform similarly (with  $\pm 0.06\%$  difference in the accuracy), and they both outperform other baselines.

We emphasize that our algorithm SuRP has an additional advantage in optimizing the bit rate of the model thanks to the rate-distortion theoretic basis of our approach. In particular, the decoder has only access to a list of indices, and these indices represent the whole (compressed) model – more efficient than describing the precise values of surviving weights. However, our current implementation does

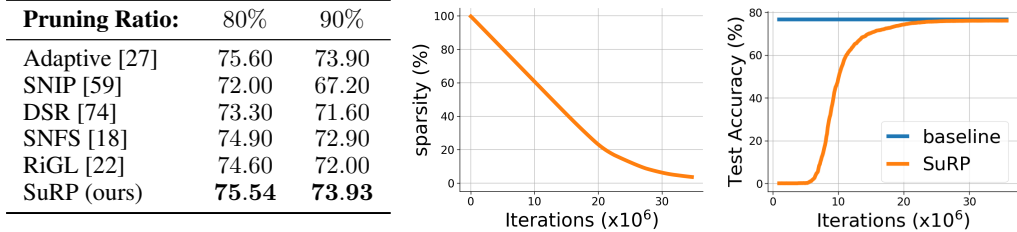


Figure 2: **(left)** Accuracy of ResNet-50 on ImageNet. Results are averaged over three runs. **(right)** Sparsity and accuracy of the reconstructed ResNet-50 on ImageNet during one cycle of SuRP. Iterations correspond to the iterations running inside SuRP.

not exploit this efficiency to the full extent due to retraining steps after each pruning iteration. Like many, we will also look for ways to prune (compress in general) NN models without a retraining step afterward. That way, SuRP can be improved to provide a better accuracy-bit rate tradeoff, together with the already demonstrated superior sparsity-accuracy tradeoff. We give more details on this and share experimental results in Appendix F and I. Finally, to give an idea about the bit rate efficiency of SuRP, we apply it for compressing gradients in a federated learning setting. Since the compressed gradients are not exposed to fine-tuning (like retraining in pruning), SuRP provides a substantial improvement on the bit rate compared to prior work. We elaborate more on this in the next paragraph.

		Pruning Ratio:	93.12%	95.60%	97.19%	98.20%	98.85%	99.26%	99.53%	99.70%	99.81%	99.88%
VGG-16	Global [73]	91.30	90.80	89.28	85.55	81.56	54.58	41.91	31.93	21.87	11.72	
	Uniform [109]	91.47	90.78	88.61	84.17	55.68	38.51	26.41	16.75	11.58	9.95	
	Adaptive [27]	91.54	91.20	90.16	89.44	87.85	86.53	84.84	82.41	74.54	24.46	
	RiGL [22]	92.34	91.99	91.66	91.15	90.55	89.51	88.21	86.73	84.85	81.50	
	LAMP [58]	92.24	92.06	91.71	91.66	91.07	90.49	89.64	88.75	87.07	84.90	
	SuRP (ours)	<b>92.55</b>	<b>92.13</b>	<b>91.95</b>	<b>91.72</b>	<b>91.21</b>	<b>90.73</b>	<b>90.65</b>	<b>89.70</b>	<b>87.28</b>	<b>85.04</b>	
		Pruning Ratio:	79.03%	86.58%	91.41%	94.50%	96.48%	97.75%	98.56%	99.08%	99.41%	99.62%
ResNet-20	Global [73]	87.48	86.97	86.29	85.02	83.15	80.52	76.28	70.69	47.47	12.02	
	Uniform [109]	87.24	86.70	86.09	84.53	82.05	77.19	64.24	47.97	20.45	13.35	
	Adaptive [27]	87.30	87.00	86.27	85.00	83.23	80.40	76.40	69.31	52.06	20.19	
	RiGL [22]	87.63	87.49	86.83	85.84	84.08	81.76	78.70	74.40	66.42	50.90	
	LAMP [58]	87.54	87.12	86.56	85.64	84.18	81.56	78.63	74.20	67.01	51.24	
	SuRP (ours)	<b>91.37</b>	<b>90.44</b>	<b>89.00</b>	<b>88.87</b>	<b>87.05</b>	<b>83.98</b>	<b>79.00</b>	<b>74.86</b>	<b>70.64</b>	<b>54.22</b>	

Table 1: Accuracy of VGG-16 and ResNet-20 on CIFAR-10. Results are averaged over five runs.

**Compression for Federated Learning (FL):** FL is a distributed training setting where edge devices are responsible for doing local training and sending local gradients to a central server [50]. Given the resource limitations of edge devices, gradient communication is a significant bottleneck in FL, and gradient compression is crucial [51]. We show in Appendix G that Laplacian distribution is a good fit for NN gradients. Therefore, SuRP is applicable to this problem as well. Our preliminary experiments with LeNet-5-Caffe on MNIST compare SuRP with DGC [63] and rTop-k [4]. We compute the communication budget for prior work by assuming a naive encoding with  $k(\log n + 32)$  bits ( $n$  is the model size) since no other method is provided. With the same sparsity ratio 99.9%, DGC achieves 98.5% accuracy with **2.05KB** of budget, rTop- $k$  achieves 99.1% accuracy with **2.05KB** of budget, and SuRP achieves 99.1% accuracy with **218B** of budget. Thus, SuRP provides 10 $\times$  times improvement in the gradients’ compression rate while achieving the same accuracy as rTop- $k$ .

## 7 Discussion and Conclusion

In this work, we connected two lines of research, namely, data compression and NN compression. In particular, we explained the compressibility of NN models via rate-distortion theory. Although our initial goal was to understand the theoretical tradeoff between the compression ratio and output perturbation, we found out that the rate-distortion theoretic formulation of the problem also introduces a theoretical foundation for pruning. Guided by this, we developed a NN compression algorithm that outputs a pruned model and outperforms prior work on CIFAR-10 and ImageNet datasets.

**Limitations:** One limitation of the proposed approach is i.i.d. source assumption. While previous score-based pruning approaches make the same assumption implicitly, empirical results indicate that NN weights are correlated, hence not independent. In future work, we plan to formalize the problem without i.i.d. assumption while also hypothesizing about the source distribution more rigorously.

**Societal Impact:** When we evaluated our strategy, we only considered accuracy as a metric. However, compression might have a negative impact on other properties of the model as well, such as fairness, as pointed out in a recent work [41]. Like many NN compression works, our distortion function does not address the potential disproportionate effects of compression on different subgroups of data. We agree that this is an issue that must attract more attention from the research community.

## 8 Acknowledgement

This work was supported in part by a Sony Stanford Graduate Fellowship.

## References

- [1] A. F. Aji and K. Heafield. Sparse communication for distributed gradient descent. *arXiv preprint arXiv:1704.05021*, 2017.
- [2] J. Ballé, V. Laparra, and E. P. Simoncelli. End-to-end optimized image compression. *arXiv preprint arXiv:1611.01704*, 2016.
- [3] R. Banner, I. Hubara, E. Hoffer, and D. Soudry. Scalable methods for 8-bit training of neural networks. In *Advances in neural information processing systems*, pages 5145–5153, 2018.
- [4] L. P. Barnes, H. A. Inan, B. Isik, and A. Ozgur. rtop-k: A statistical estimation approach to distributed sgd. *arXiv preprint arXiv:2005.10761*, 2020.
- [5] T. Berger. Rate-distortion theory. *Wiley Encyclopedia of Telecommunications*, 2003.
- [6] D. Blalock, J. J. G. Ortiz, J. Frankle, and J. Guttag. What is the state of neural network pruning? *arXiv preprint arXiv:2003.03033*, 2020.
- [7] C. Bucilua, R. Caruana, and A. Niculescu-Mizil. Model compression. In *Proceedings of the 12th ACM SIGKDD International Conference on Knowledge Discovery and Data Mining*, KDD ’06, page 535–541, New York, NY, USA, 2006. Association for Computing Machinery. ISBN 1595933395. doi: 10.1145/1150402.1150464. URL <https://doi.org/10.1145/1150402.1150464>.
- [8] M. A. Carreira-Perpinan and Y. Idelbayev. “learning-compression” algorithms for neural net pruning. In *Proceedings of the IEEE Conference on Computer Vision and Pattern Recognition*, pages 8532–8541, 2018.
- [9] G. Castellano, A. M. Fanelli, and M. Pelillo. An iterative pruning algorithm for feedforward neural networks. *IEEE transactions on Neural networks*, 8(3):519–531, 1997.
- [10] T. Chen, Z. Zhang, S. Liu, S. Chang, and Z. Wang. Long live the lottery: The existence of winning tickets in lifelong learning. In *International Conference on Learning Representations, 2021a*. URL <https://openreview.net/forum>, 2021.
- [11] Y. Cheng, D. Wang, P. Zhou, and T. Zhang. Model compression and acceleration for deep neural networks: The principles, progress, and challenges. *IEEE Signal Processing Magazine*, 35(1):126–136, 2018.
- [12] Y. Choi, M. El-Khamy, and J. Lee. Universal deep neural network compression. *IEEE Journal of Selected Topics in Signal Processing*, 2020.
- [13] T. M. Cover and J. A. Thomas. *Elements of Information Theory (Wiley Series in Telecommunications and Signal Processing)*. Wiley-Interscience, USA, 2006. ISBN 0471241954.
- [14] Y. L. Cun, J. S. Denker, and S. A. Solla. *Optimal Brain Damage*, page 598–605. Morgan Kaufmann Publishers Inc., San Francisco, CA, USA, 1990. ISBN 1558601007.

[15] B. Dai, C. Zhu, B. Guo, and D. Wipf. Compressing neural networks using the variational information bottleneck. In J. Dy and A. Krause, editors, *Proceedings of the 35th International Conference on Machine Learning*, volume 80 of *Proceedings of Machine Learning Research*, pages 1135–1144. PMLR, 10–15 Jul 2018. URL <http://proceedings.mlr.press/v80/dai18d.html>.

[16] J. Dean, G. Corrado, R. Monga, K. Chen, M. Devin, M. Mao, M. Ranzato, A. Senior, P. Tucker, K. Yang, et al. Large scale distributed deep networks. In *Advances in neural information processing systems*, pages 1223–1231, 2012.

[17] J. Deng, W. Dong, R. Socher, L.-J. Li, K. Li, and L. Fei-Fei. ImageNet: A Large-Scale Hierarchical Image Database. In *CVPR09*, 2009.

[18] T. Dettmers and L. Zettlemoyer. Sparse networks from scratch: Faster training without losing performance. *arXiv preprint arXiv:1907.04840*, 2019.

[19] E. Elsen, M. Dukhan, T. Gale, and K. Simonyan. Fast sparse convnets. In *Proceedings of the IEEE/CVF conference on computer vision and pattern recognition*, pages 14629–14638, 2020.

[20] A. P. Engelbrecht. A new pruning heuristic based on variance analysis of sensitivity information. *IEEE transactions on Neural Networks*, 12(6):1386–1399, 2001.

[21] W. H. Equitz and T. M. Cover. Successive refinement of information. *IEEE Transactions on Information Theory*, 37(2):269–275, 1991.

[22] U. Evci, T. Gale, J. Menick, P. S. Castro, and E. Elsen. Rigging the lottery: Making all tickets winners. In *International Conference on Machine Learning*, pages 2943–2952. PMLR, 2020.

[23] M. Federici, K. Ullrich, and M. Welling. Improved bayesian compression. *arXiv preprint arXiv:1711.06494*, 2017.

[24] J. Frankle and M. Carbin. The lottery ticket hypothesis: Finding sparse, trainable neural networks. *International Conference on Learning Representations (ICLR)*, 2019.

[25] J. Frankle, G. K. Dziugaite, D. Roy, and M. Carbin. Linear mode connectivity and the lottery ticket hypothesis. In *International Conference on Machine Learning*, pages 3259–3269. PMLR, 2020.

[26] J. Frankle, G. K. Dziugaite, D. M. Roy, and M. Carbin. Pruning neural networks at initialization: Why are we missing the mark? *arXiv preprint arXiv:2009.08576*, 2020.

[27] T. Gale, E. Elsen, and S. Hooker. The state of sparsity in deep neural networks. *arXiv preprint arXiv:1902.09574*, 2019.

[28] T. Gale, M. Zaharia, C. Young, and E. Elsen. Sparse gpu kernels for deep learning. *arXiv preprint arXiv:2006.10901*, 2020.

[29] R. Gallager and D. Van Voorhis. Optimal source codes for geometrically distributed integer alphabets (corresp.). *IEEE Transactions on Information theory*, 21(2):228–230, 1975.

[30] W. Gao, Y.-H. Liu, C. Wang, and S. Oh. Rate distortion for model compression: From theory to practice. In *International Conference on Machine Learning*, pages 2102–2111. PMLR, 2019.

[31] S. Golomb. Run-length encodings (corresp.). *IEEE transactions on information theory*, 12(3):399–401, 1966.

[32] J. Gou, B. Yu, S. J. Maybank, and D. Tao. Knowledge distillation: A survey. *International Journal of Computer Vision*, pages 1–31, 2021.

[33] P. D. Grünwald and A. Grunwald. *The minimum description length principle*. MIT press, 2007.

[34] Y. Guo, A. Yao, and Y. Chen. Dynamic network surgery for efficient dnns. In *Advances in neural information processing systems*, pages 1379–1387, 2016.

- [35] S. Han, J. Pool, J. Tran, and W. Dally. Learning both weights and connections for efficient neural network. In *Advances in neural information processing systems*, pages 1135–1143, 2015.
- [36] S. Han, H. Mao, and W. J. Dally. Deep compression: Compressing deep neural networks with pruning, trained quantization and huffman coding. *International Conference on Learning Representations (ICLR)*, 2016.
- [37] B. Hassibi, D. G. Stork, G. Wolff, and T. Watanabe. Optimal brain surgeon: Extensions and performance comparisons. In *Proceedings of the 6th International Conference on Neural Information Processing Systems*, NIPS’93, page 263–270, San Francisco, CA, USA, 1993.
- [38] M. Havasi, R. Peharz, and J. M. Hernández-Lobato. Minimal random code learning: Getting bits back from compressed model parameters. In *International Conference on Learning Representations (ICLR)*, 2019.
- [39] K. He, X. Zhang, S. Ren, and J. Sun. Deep residual learning for image recognition. In *Proceedings of the IEEE conference on computer vision and pattern recognition*, pages 770–778, 2016.
- [40] G. Hinton, O. Vinyals, and J. Dean. Distilling the knowledge in a neural network. In *NIPS Deep Learning and Representation Learning Workshop*, 2015. URL <http://arxiv.org/abs/1503.02531>.
- [41] S. Hooker, N. Moorosi, G. Clark, S. Bengio, and E. Denton. Characterising bias in compressed models. *arXiv preprint arXiv:2010.03058*, 2020.
- [42] D. A. Huffman. A method for the construction of minimum-redundancy codes. *Proceedings of the IRE*, 40(9):1098–1101, 1952.
- [43] Y. Idelbayev and M. A. Carreira-Perpinan. Low-rank compression of neural nets: Learning the rank of each layer. In *Proceedings of the IEEE/CVF Conference on Computer Vision and Pattern Recognition (CVPR)*, June 2020.
- [44] Y. Idelbayev and M. A. Carreira-Perpinan. Neural network compression via additive combination of reshaped, low-rank matrices. In *2021 Data Compression Conference (DCC)*, pages 243–252, 2021. doi: 10.1109/DCC50243.2021.00032.
- [45] Y. Idelbayev, P. Molchanov, M. Shen, H. Yin, M. A. Carreira-Perpinan, and J. M. Alvarez. Optimal quantization using scaled codebook. In *Proc. of the 2021 IEEE Computer Society Conf. Computer Vision and Pattern Recognition (CVPR’21), Virtual*, 2021.
- [46] Y. Ioannou, D. Robertson, J. Shotton, R. Cipolla, and A. Criminisi. Training cnns with low-rank filters for efficient image classification. *arXiv preprint arXiv:1511.06744*, 2015.
- [47] B. Isik, K. Choi, X. Zheng, T. Weissman, S. Ermon, H. S. P. Wong, and A. Alaghi. Neural network compression for noisy storage devices. *arXiv preprint arXiv:2102.07725*, 2021.
- [48] B. Jacob, S. Kligys, B. Chen, M. Zhu, M. Tang, A. Howard, H. Adam, and D. Kalenichenko. Quantization and training of neural networks for efficient integer-arithmetic-only inference. In *Proceedings of the IEEE Conference on Computer Vision and Pattern Recognition*, pages 2704–2713, 2018.
- [49] S. Jung, C. Son, S. Lee, J. Son, J.-J. Han, Y. Kwak, S. J. Hwang, and C. Choi. Learning to quantize deep networks by optimizing quantization intervals with task loss. In *Proceedings of the IEEE/CVF Conference on Computer Vision and Pattern Recognition*, pages 4350–4359, 2019.
- [50] P. Kairouz, H. B. McMahan, B. Avent, A. Bellet, M. Bennis, A. N. Bhagoji, K. Bonawitz, Z. Charles, G. Cormode, R. Cummings, et al. Advances and open problems in federated learning. *arXiv preprint arXiv:1912.04977*, 2019.
- [51] J. Konečný, H. B. McMahan, F. X. Yu, P. Richtarik, A. T. Suresh, and D. Bacon. Federated learning: Strategies for improving communication efficiency. In *NIPS Workshop on Private Multi-Party Machine Learning*, 2016.

[52] V. N. Koshelev. Hierarchical coding of discrete sources. *Problemy peredachi informatsii*, 16(3):31–49, 1980.

[53] A. Krizhevsky, G. Hinton, et al. Learning multiple layers of features from tiny images. 2009.

[54] A. Kusupati, V. Ramanujan, R. Soman, M. Wortsman, P. Jain, S. Kakade, and A. Farhadi. Soft threshold weight reparameterization for learnable sparsity. In *International Conference on Machine Learning*, pages 5544–5555. PMLR, 2020.

[55] Y. LeCun, L. Bottou, Y. Bengio, and P. Haffner. Gradient-based learning applied to document recognition. *Proceedings of the IEEE*, 86(11):2278–2324, 1998.

[56] Y. LeCun, C. Cortes, and C. Burges. Mnist handwritten digit database, 2010.

[57] Y. LeCun, Y. Bengio, and G. Hinton. Deep learning. *nature*, 521(7553):436–444, 2015.

[58] J. Lee, S. Park, S. Mo, S. Ahn, and J. Shin. Layer-adaptive sparsity for the magnitude-based pruning. *International Conference on Learning Representations*, 2021.

[59] N. Lee, T. Ajanthan, and P. H. Torr. Snip: Single-shot network pruning based on connection sensitivity. *arXiv preprint arXiv:1810.02340*, 2018.

[60] F. Li, B. Zhang, and B. Liu. Ternary weight networks. *arXiv preprint arXiv:1605.04711*, 2016.

[61] J. Lin, Y. Rao, J. Lu, and J. Zhou. Runtime neural pruning. In *Proceedings of the 31st International Conference on Neural Information Processing Systems*, pages 2178–2188, 2017.

[62] S. Lin, R. Ji, C. Yan, B. Zhang, L. Cao, Q. Ye, F. Huang, and D. Doermann. Towards optimal structured cnn pruning via generative adversarial learning. In *Proceedings of the IEEE/CVF Conference on Computer Vision and Pattern Recognition*, pages 2790–2799, 2019.

[63] Y. Lin, S. Han, H. Mao, Y. Wang, and W. J. Dally. Deep gradient compression: Reducing the communication bandwidth for distributed training. *International Conference on Learning Representations (ICLR)*, 2017.

[64] Z. Liu, M. Sun, T. Zhou, G. Huang, and T. Darrell. Rethinking the value of network pruning. *arXiv preprint arXiv:1810.05270*, 2018.

[65] Z. Liu, J. Xu, X. Peng, and R. Xiong. Frequency-domain dynamic pruning for convolutional neural networks. In *Proceedings of the 32nd International Conference on Neural Information Processing Systems*, pages 1051–1061, 2018.

[66] Z. Liu, H. Mu, X. Zhang, Z. Guo, X. Yang, K.-T. Cheng, and J. Sun. Metapruning: Meta learning for automatic neural network channel pruning. In *Proceedings of the IEEE/CVF International Conference on Computer Vision*, pages 3296–3305, 2019.

[67] C. Louizos, K. Ullrich, and M. Welling. Bayesian compression for deep learning. *arXiv preprint arXiv:1705.08665*, 2017.

[68] C. Louizos, M. Welling, and D. P. Kingma. Learning sparse neural networks through  $l_0$  regularization. *arXiv preprint arXiv:1712.01312*, 2017.

[69] H. B. McMahan, E. Moore, D. Ramage, S. Hampson, and B. A. y Arcas. Communication-efficient learning of deep networks from decentralized data. In *AISTATS*, 2017.

[70] D. C. Mocanu, E. Mocanu, P. Stone, P. H. Nguyen, M. Gibescu, and A. Liotta. Scalable training of artificial neural networks with adaptive sparse connectivity inspired by network science. *Nature communications*, 9(1):1–12, 2018.

[71] D. Molchanov, A. Ashukha, and D. Vetrov. Variational dropout sparsifies deep neural networks. In *International Conference on Machine Learning*, pages 2498–2507. PMLR, 2017.

[72] P. Molchanov, S. Tyree, T. Karras, T. Aila, and J. Kautz. Pruning convolutional neural networks for resource efficient inference. *arXiv preprint arXiv:1611.06440*, 2016.

- [73] A. S. Morcos, H. Yu, M. Paganini, and Y. Tian. One ticket to win them all: generalizing lottery ticket initializations across datasets and optimizers. *arXiv preprint arXiv:1906.02773*, 2019.
- [74] H. Mostafa and X. Wang. Parameter efficient training of deep convolutional neural networks by dynamic sparse reparameterization. In *International Conference on Machine Learning*, pages 4646–4655. PMLR, 2019.
- [75] A. No and T. Weissman. Rateless lossy compression via the extremes. *IEEE transactions on information theory*, 62(10):5484–5495, 2016.
- [76] A. No, A. Ingber, and T. Weissman. Strong successive refinability and rate-distortion-complexity tradeoff. *IEEE Transactions on Information Theory*, 62(6):3618–3635, 2016.
- [77] D. Oktay, J. Ballé, S. Singh, and A. Shrivastava. Scalable model compression by entropy penalized reparameterization. In *International Conference on Learning Representations (ICLR)*, 2019.
- [78] S. Park, J. Lee, S. Mo, and J. Shin. Lookahead: A far-sighted alternative of magnitude-based pruning. *International Conference on Learning Representations (ICLR)*, 2020.
- [79] A. Paszke, S. Gross, F. Massa, A. Lerer, J. Bradbury, G. Chanan, T. Killeen, Z. Lin, N. Gimelshein, L. Antiga, A. Desmaison, A. Kopf, E. Yang, Z. DeVito, M. Raison, A. Tejani, S. Chilamkurthy, B. Steiner, L. Fang, J. Bai, and S. Chintala. Pytorch: An imperative style, high-performance deep learning library. In H. Wallach, H. Larochelle, A. Beygelzimer, F. d’Alché-Buc, E. Fox, and R. Garnett, editors, *Advances in Neural Information Processing Systems 32*, pages 8024–8035. Curran Associates, Inc., 2019.
- [80] H. Peng, J. Wu, S. Chen, and J. Huang. Collaborative channel pruning for deep networks. In *International Conference on Machine Learning*, pages 5113–5122. PMLR, 2019.
- [81] A. Polino, R. Pascanu, and D. Alistarh. Model compression via distillation and quantization. *arXiv preprint arXiv:1802.05668*, 2018.
- [82] A. Renda, J. Frankle, and M. Carbin. Comparing fine-tuning and rewinding in neural network pruning. In *International Conference on Learning Representations*, 2020.
- [83] T. N. Sainath, B. Kingsbury, V. Sindhwan, E. Arisoy, and B. Ramabhadran. Low-rank matrix factorization for deep neural network training with high-dimensional output targets. In *2013 IEEE international conference on acoustics, speech and signal processing*, pages 6655–6659. IEEE, 2013.
- [84] D. Salomon. *Data compression: the complete reference*. Springer Science & Business Media, 2004.
- [85] V. Sehwag, S. Wang, P. Mittal, and S. Jana. Hydra: Pruning adversarially robust neural networks. *Advances in Neural Information Processing Systems (NeurIPS)*, 7, 2020.
- [86] C. E. Shannon. Coding theorems for a discrete source with a fidelity criterion. *IRE Nat. Conv. Rec*, 4(142-163):1, 1959.
- [87] C. E. Shannon. A mathematical theory of communication. *ACM SIGMOBILE mobile computing and communications review*, 5(1):3–55, 2001.
- [88] K. Simonyan and A. Zisserman. Very deep convolutional networks for large-scale image recognition. *arXiv preprint arXiv:1409.1556*, 2014.
- [89] S. P. Singh and D. Alistarh. Woodfisher: Efficient second-order approximations for model compression. *arXiv preprint arXiv:2004.14340*, 2020.
- [90] S. Srinivas and R. V. Babu. Data-free parameter pruning for deep neural networks. *arXiv preprint arXiv:1507.06149*, 2015.
- [91] P. Stock, A. Fan, B. Graham, E. Grave, R. Gribonval, H. Jegou, and A. Joulin. Training with quantization noise for extreme model compression. In *International Conference on Learning Representations*, 2021. URL <https://openreview.net/forum?id=dV19Yyi1fS3>.

[92] K. Ullrich, E. Meeds, and M. Welling. Soft weight-sharing for neural network compression. *arXiv preprint arXiv:1702.04008*, 2017.

[93] R. Venkataraman, T. Sarkar, and S. Tatikonda. Lossy compression via sparse linear regression: Computationally efficient encoding and decoding. *IEEE transactions on information theory*, 60(6):3265–3278, 2014.

[94] S. Verdu. The exponential distribution in information theory. *Problemy peredachi informatsii*, 32(1):100–111, 1996.

[95] H. Wang, S. Sievert, S. Liu, Z. B. Charles, D. S. Papailiopoulos, and S. Wright. Atomo: Communication-efficient learning via atomic sparsification. In *NeurIPS*, 2018.

[96] J. Wang, W. Bao, L. Sun, X. Zhu, B. Cao, and S. Y. Philip. Private model compression via knowledge distillation. In *Proceedings of the AAAI Conference on Artificial Intelligence*, volume 33, pages 1190–1197, 2019.

[97] K. Wang, Z. Liu, Y. Lin, J. Lin, and S. Han. Haq: Hardware-aware automated quantization with mixed precision. In *Proceedings of the IEEE/CVF Conference on Computer Vision and Pattern Recognition*, pages 8612–8620, 2019.

[98] Y. Wang, X. Zhang, L. Xie, J. Zhou, H. Su, B. Zhang, and X. Hu. Pruning from scratch. In *Proceedings of the AAAI Conference on Artificial Intelligence*, volume 34, pages 12273–12280, 2020.

[99] J. Wangni, J. Wang, J. Liu, and T. Zhang. Gradient sparsification for communication-efficient distributed optimization. In S. Bengio, H. Wallach, H. Larochelle, K. Grauman, N. Cesa-Bianchi, and R. Garnett, editors, *Advances in Neural Information Processing Systems 31*, pages 1299–1309. Curran Associates, Inc., 2018.

[100] S. Wiedemann, H. Kirchhoffer, S. Matlage, P. Haase, A. Marban, T. Marinč, D. Neumann, T. Nguyen, H. Schwarz, T. Wiegand, D. Marpe, and W. Samek. Deepcabac: A universal compression algorithm for deep neural networks. *IEEE Journal of Selected Topics in Signal Processing*, 14(4):700–714, 2020.

[101] P. M. Williams. Bayesian regularization and pruning using a laplace prior. *Neural computation*, 7(1):117–143, 1995.

[102] X. Xiao, Z. Wang, and S. Rajasekaran. Autoprune: Automatic network pruning by regularizing auxiliary parameters. *Advances in neural information processing systems*, 32, 2019.

[103] T.-J. Yang, Y.-H. Chen, and V. Sze. Designing energy-efficient convolutional neural networks using energy-aware pruning. In *Proceedings of the IEEE Conference on Computer Vision and Pattern Recognition (CVPR)*, July 2017.

[104] P. Yin, S. Zhang, J. Lyu, S. Osher, Y. Qi, and J. Xin. Binaryrelax: A relaxation approach for training deep neural networks with quantized weights. *SIAM Journal on Imaging Sciences*, 11(4):2205–2223, 2018.

[105] S. I. Young, W. Zhe, D. Taubman, and B. Girod. Transform quantization for cnn compression. *arXiv preprint arXiv:2009.01174*, 2020.

[106] R. Yu, A. Li, C.-F. Chen, J.-H. Lai, V. I. Morariu, X. Han, M. Gao, C.-Y. Lin, and L. S. Davis. Nisp: Pruning networks using neuron importance score propagation. In *Proceedings of the IEEE Conference on Computer Vision and Pattern Recognition*, pages 9194–9203, 2018.

[107] C. Zhao, B. Ni, J. Zhang, Q. Zhao, W. Zhang, and Q. Tian. Variational convolutional neural network pruning. In *Proceedings of the IEEE/CVF Conference on Computer Vision and Pattern Recognition*, pages 2780–2789, 2019.

[108] W. Zhe, J. Lin, M. S. Aly, S. Young, V. Chandrasekhar, and B. Girod. Rate-distortion optimized coding for efficient cnn compression. In *2021 Data Compression Conference (DCC)*, pages 253–262. IEEE, 2021.

[109] M. Zhu and S. Gupta. To prune, or not to prune: exploring the efficacy of pruning for model compression. *arXiv preprint arXiv:1710.01878*, 2017.

## Appendix

### A Proof of Theorem 1

In this section, we provide the proof of Theorem 1. The fully connected  $d$ -layer NN model with 1-Lipschitz activations  $\sigma(\cdot)$  is given by

$$f(\mathbf{x}; \mathbf{w}) = \mathbf{w}^{(d)} \sigma(\mathbf{w}^{(d-1)} \sigma(\dots \mathbf{w}^{(2)} \sigma(\mathbf{w}^{(1)} \mathbf{x}))).$$

We let  $\mathbf{w}^{(1:i)} = \{\mathbf{w}^{(1)}, \dots, \mathbf{w}^{(i)}\}$  for  $1 \leq i \leq d$  where  $\mathbf{w}^{(1:d)} = \mathbf{w}$ . Furthermore, we define the first  $i$  layer of the network by

$$f(\mathbf{x}; \mathbf{w}^{(1:i)}) = \mathbf{w}^{(i)} \sigma(\mathbf{w}^{(i-1)} \sigma(\dots \mathbf{w}^{(2)} \sigma(\mathbf{w}^{(1)} \mathbf{x}))).$$

Then, the output perturbation is bounded by

$$\begin{aligned} & \|f(\mathbf{x}; \mathbf{w}^{(1:d)}) - f(\mathbf{x}; \hat{\mathbf{w}}^{(1:d)})\|_1 \\ &= \|\mathbf{w}^{(d)} \sigma(f(\mathbf{x}; \mathbf{w}^{(1:d-1)})) - \hat{\mathbf{w}}^{(d)} \sigma(f(\mathbf{x}; \hat{\mathbf{w}}^{(1:d-1)}))\|_1 \\ &\leq \|\mathbf{w}^{(d)} \sigma(f(\mathbf{x}; \mathbf{w}^{(1:d-1)})) - \hat{\mathbf{w}}^{(d)} \sigma(f(\mathbf{x}; \mathbf{w}^{(1:d-1)}))\|_1 \\ &\quad + \|\hat{\mathbf{w}}^{(d)} \sigma(f(\mathbf{x}; \mathbf{w}^{(1:d-1)})) - \hat{\mathbf{w}}^{(d)} \sigma(f(\mathbf{x}; \hat{\mathbf{w}}^{(1:d-1)}))\|_1 \end{aligned} \quad (10)$$

$$\leq \|\mathbf{w}^{(d)} - \hat{\mathbf{w}}^{(d)}\|_1 \cdot \|\sigma(f(\mathbf{x}; \mathbf{w}^{(1:d-1)}))\|_1 + \|\hat{\mathbf{w}}^{(d)}\|_1 \cdot \|\sigma(f(\mathbf{x}; \mathbf{w}^{(1:d-1)})) - \sigma(f(\mathbf{x}; \hat{\mathbf{w}}^{(1:d-1)}))\|_1 \quad (11)$$

$$\leq \|\mathbf{w}^{(d)} - \hat{\mathbf{w}}^{(d)}\|_1 \cdot \|f(\mathbf{x}; \mathbf{w}^{(1:d-1)})\|_1 + \|\hat{\mathbf{w}}^{(d)}\|_1 \cdot \|f(\mathbf{x}; \mathbf{w}^{(1:d-1)}) - f(\mathbf{x}; \hat{\mathbf{w}}^{(1:d-1)})\|_1 \quad (12)$$

$$\leq \|\mathbf{w}^{(d)} - \hat{\mathbf{w}}^{(d)}\|_1 \cdot \prod_{l=1}^{d-1} \|\mathbf{w}^{(l)}\|_1 \cdot \|\mathbf{x}\|_1 + \|\hat{\mathbf{w}}^{(d)}\|_1 \cdot \|f(\mathbf{x}; \mathbf{w}^{(1:d-1)}) - f(\mathbf{x}; \hat{\mathbf{w}}^{(1:d-1)})\|_1 \quad (13)$$

$$\leq \|\mathbf{w}^{(d)} - \hat{\mathbf{w}}^{(d)}\|_1 \cdot \prod_{l=1}^{d-1} \|\mathbf{w}^{(l)}\|_1 + \|\hat{\mathbf{w}}^{(d)}\|_1 \cdot \|f(\mathbf{x}; \mathbf{w}^{(1:d-1)}) - f(\mathbf{x}; \hat{\mathbf{w}}^{(1:d-1)})\|_1 \quad (14)$$

$$\leq \|\mathbf{w}^{(d)} - \hat{\mathbf{w}}^{(d)}\|_1 \cdot \prod_{l=1}^{d-1} \|\mathbf{w}^{(l)}\|_1 + \|\mathbf{w}^{(d)}\|_1 \cdot \|f(\mathbf{x}; \mathbf{w}^{(1:d-1)}) - f(\mathbf{x}; \hat{\mathbf{w}}^{(1:d-1)})\|_1 \quad (15)$$

where Eq. 10 is due to triangle inequality, and Eq. 11 holds from the property of  $\ell_1$ -norm (and induced norm). Eq. 12 is from 1-Lipshitzness of activation  $\sigma(\cdot)$ , i.e.,  $\|\sigma(\mathbf{x})\|_1 \leq \|\mathbf{x}\|_1$ . Eq. 13 holds from the following lemma.

**Lemma 2.** For all  $1 \leq i \leq d$ , we have  $\|f(\mathbf{x}; \mathbf{w}^{(1:i)})\|_1 \leq \prod_{j=1}^i \|\mathbf{w}^{(j)}\|_1 \cdot \|\mathbf{x}\|_1$ .

*Proof.* From the property of  $\ell_1$ -norm, we have

$$\|f(\mathbf{x}; \mathbf{w}^{(1:i)})\|_1 \leq \|\mathbf{w}^{(i)}\|_1 \cdot \|\sigma(f(\mathbf{x}; \mathbf{w}^{(1:i-1)}))\|_1 \quad (16)$$

$$\leq \|\mathbf{w}^{(i)}\|_1 \cdot \|f(\mathbf{x}; \mathbf{w}^{(1:i-1)})\|_1 \quad (17)$$

where the last inequality is due to 1-Lipshitzness of  $\sigma$ . Then, we can keep applying the same inequality, which concludes the proof.  $\square$

Eq. 14 follows by the constraint  $\|\mathbf{x}\|_1 \leq 1$  in Theorem 1. Finally Eq. 15 is from the assumption  $\|\hat{\mathbf{w}}^{(l)}\|_1 \leq \|\mathbf{w}^{(l)}\|_1$  for all  $1 \leq l \leq d$ .

Thus, we have

$$\begin{aligned} & \left( \prod_{l=1}^d \frac{1}{\|\mathbf{w}^{(l)}\|_1} \right) \|f(\mathbf{x}; \mathbf{w}^{(1:d)}) - f(\mathbf{x}; \hat{\mathbf{w}}^{(1:d)})\|_1 \\ & \leq \frac{\|\mathbf{w}^{(d)} - \hat{\mathbf{w}}^{(d)}\|_1}{\|\mathbf{w}^{(d)}\|_1} + \left( \prod_{l=1}^{d-1} \frac{1}{\|\mathbf{w}^{(l)}\|_1} \right) \|f(\mathbf{x}; \mathbf{w}^{(1:d-1)}) - f(\mathbf{x}; \hat{\mathbf{w}}^{(1:d-1)})\|_1. \end{aligned} \quad (18)$$

We can repeat the same procedure, and get

$$\begin{aligned} & \left( \prod_{l=1}^d \frac{1}{\|\mathbf{w}^{(l)}\|_1} \right) \|f(\mathbf{x}; \mathbf{w}^{(1:d)}) - f(\mathbf{x}; \hat{\mathbf{w}}^{(1:d)})\|_1 \\ & \leq \sum_{l=1}^d \frac{\|\mathbf{w}^{(l)} - \hat{\mathbf{w}}^{(l)}\|_1}{\|\mathbf{w}^{(l)}\|_1}. \end{aligned} \quad (19)$$

This completes the proof.

## B Density Estimation for Neural Network Parameters without Normalization

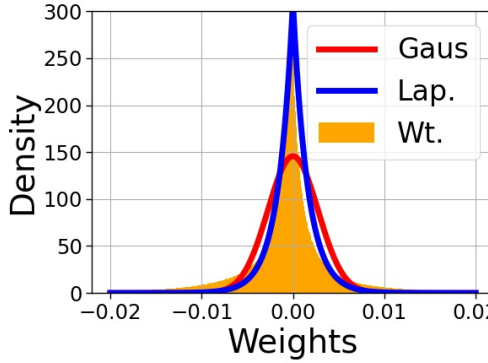


Figure 3: Weight Density of ResNet-18 (trained on CIFAR-10) before normalization.

In Section 4, we have justified our assumption of Laplacian distribution over normalized NN weights through density plots for three distinct architectures. We have also emphasized that Laplacian would be a good fit for unnormalized NN weights as well. We give the density plots of unnormalized weights of ResNet-18 in Figure 3 to justify our claim empirically. This claim implies that SuRP can also be applied to NNs without normalization and it would achieve rate-distortion theoretic optimal performance for reconstructing the NN weights back. However, recall from Theorem 1 that  $\ell_1$  distortion of normalized weights upper bounds the output perturbation. Since we care more about maintaining the outputs rather than the weights themselves, we have applied SuRP after the normalization.

We have additionally observed that weights of layers closer to the input tend to follow a Gaussian-like distribution. In contrast, the weights of layers closer to the output behave like Laplacian random variables. Since the last layers have larger number of parameters in the architectures used in this work, we see a Laplacian distribution over the weights globally. Therefore, different pruning strategies might be necessary for layers with Gaussian and Laplacian behaviour for a layer by layer pruning approach.

## C Proof of Lemma 1

In this section, we briefly describe the proof outline of Lemma 1 in Section 4, which is provided in [5]. Consider the Laplacian source  $U \sim P_U$  with parameter  $\lambda$ , and the target distortion  $D$  satisfies  $0 \leq D \leq 1/\lambda$ . Then,

$$\begin{aligned} R(D) &= \min_{\mathbb{E}[d(U, \hat{U})] \leq D} I(U; \hat{U}) \\ &= \inf_{\mathbb{E}[|U - \hat{U}|] \leq D} I(U; \hat{U}). \end{aligned}$$

Let  $Q$  be another conditional distribution where  $Q_{U|\hat{U}}(u|\hat{u}) = \frac{1}{D}e^{-|u-\hat{u}|/D}$ . Then,

$$\begin{aligned} I(U; \hat{U}) &= D_{KL}(P_{U|\hat{U}} \| P_U | P_{\hat{U}}) \\ &= D_{KL}(P_{U|\hat{U}} \| Q_{U|\hat{U}} | P_{\hat{U}}) + \mathbb{E}_{P_{U,\hat{U}}} \left[ \log \frac{Q_{U|\hat{U}}(U|\hat{U})}{P_U(U)} \right] \\ &\geq \mathbb{E}_{P_{U,\hat{U}}} \left[ \log \frac{Q_{U|\hat{U}}(U|\hat{U})}{P_U(U)} \right] \end{aligned} \quad (20)$$

$$\begin{aligned} &= -\log(\lambda D) - \frac{1}{D} \mathbb{E}[|U - \hat{U}|] + \lambda \mathbb{E}[|U|] \\ &\geq -\log(\lambda D) \end{aligned} \quad (21)$$

where Eq. 20 is due to nonnegativity of KL divergence, and Eq. 21 is because  $\mathbb{E}[|U|] = \frac{1}{\lambda}$  and  $\mathbb{E}[|U - \hat{U}|] \leq D$ . This implies that  $R(D) \geq -\log(\lambda D)$ . We note that we followed a technique inspired by Verdu's proof for rate-distortion function of exponential source [94]. The same lower bound can also be achieved via Shannon lower bound (SLB) [86].

On the other hand, we need to show that the lower bound  $R(D) \geq -\log(\lambda D)$  is indeed tight. Let  $V$  be a mixture of point measure and Laplacian random variable, where the probability density function is given by

$$P_V(v) = \lambda^2 D^2 \cdot \delta(v) + (1 - \lambda^2 D^2) \cdot \frac{\lambda}{2} e^{-\lambda|v|}.$$

We further let  $N$  be a Laplacian random variable with parameter  $1/D$ , where  $V$  and  $N$  are independent. Then, the Laplace transform of  $P_V$  and  $P_N$  are given by

$$\begin{aligned} \mathbb{E}[e^{-sV}] &= \lambda^2 D^2 + (1 - \lambda^2 D^2) \frac{\lambda^2}{\lambda^2 + s^2} \\ \mathbb{E}[e^{-sN}] &= \frac{1/D^2}{1/D^2 + s^2}. \end{aligned}$$

Consider the sum of two random variables  $V + N$ . Since they are independent, Laplace transform of the density of  $V + N$  is a product of the above two terms.

$$\begin{aligned} \mathbb{E}[e^{-s(V+N)}] &= \mathbb{E}[e^{-sV}] \cdot \mathbb{E}[e^{-sN}] \\ &= \frac{\lambda^2}{\lambda^2 + s^2}. \end{aligned}$$

Since it coincides with the Laplace transform of  $P_U$ , we conclude that  $U \stackrel{(d)}{=} V + N$ . Thus, by letting  $U = V + N$ , we obtain the conditional distribution  $Q_{U|V}(u|v) = \frac{1}{D}e^{-|u-v|/D}$ . It is clear that  $Q_{U|V}$  satisfies the equality conditions in Eq. 20 and Eq. 21, and therefore it achieves the lower bound  $I(U; \hat{U}) = -\log(\lambda D)$  with  $\hat{U} = V$ .

To sum, the optimal rate-distortion tradeoff is  $R(D) = -\log(\lambda D)$  and it can be achieved with a reconstruction that follows

$$P_V(v) = \lambda^2 D^2 \cdot \delta(v) + (1 - \lambda^2 D^2) \cdot \frac{\lambda}{2} e^{-\lambda|v|}. \quad (22)$$

## D Algorithms

We give the algorithm described in Section 5 in Algorithm 1. For the experiments in Section 6, we slightly modified Algorithm 1 and used Algorithm 2.

As mentioned in Section 6, these two algorithms are equivalent except the fact that Algorithm 2 applies the same compression scheme after taking the absolute value of the normalized weights. Furthermore, Algorithm 2 is rate-distortion theoretic optimal too. To see this, it is enough to follow the same steps in Sections 4 and 5 for exponential source instead of Laplacian source since the magnitude of Laplacian source sequence follows an exponential distribution. We now give the

---

**Algorithm 1** SuRP

---

**Hyperparameters:**  $\beta$ 
**Inputs:** weights  $w_1, \dots, w_n$  in  $d$  layers

**Output:** reconstructed weights  $w_1^{recon}, \dots, w_n^{recon}$ 
**Normalization:**
**for**  $l = 1, \dots, d$  **do**

$$u^{(l)} \leftarrow \frac{w^{(l)}}{\|w^{(l)}\|_1}$$

**end for**

$$(u_1^{recon}, \dots, u_n^{recon}) \leftarrow 0$$

$$\lambda \leftarrow \text{ParamEst}((u_1, \dots, u_n))$$

Encoder sends  $\lambda$  to the Decoder.

**for**  $t = 1, \dots, L$  **do**
**Encoder:**

$$m_{max} \leftarrow (\text{indices of the components in } (u_1, \dots, u_n) \text{ that are larger than } \frac{1}{\lambda} \cdot \log \frac{n}{2\beta})$$

$$m_{min} \leftarrow (\text{indices of the components in } (u_1, \dots, u_n) \text{ that are smaller than } -\frac{1}{\lambda} \cdot \log \frac{n}{2\beta})$$

**if**  $m_{max}$  or  $m_{min}$  is empty **then**

$$\lambda \leftarrow \text{ParamEst}((u_1, \dots, u_n))$$

sends  $\lambda$  to the Decoder.

**end if**

$$m_1 \leftarrow (\text{a random index from } m_{max})$$

$$m_{-1} \leftarrow (\text{a random index from } m_{min})$$

sends  $m_1$  and  $m_{-1}$  to the Decoder.

$$u_{m_1} = u_{m_1} - \frac{1}{\lambda} \cdot \log \frac{n}{2\beta}$$

$$u_{m_{-1}} = u_{m_{-1}} + \frac{1}{\lambda} \cdot \log \frac{n}{2\beta}$$

$$\lambda \leftarrow \frac{n}{n-2 \log \frac{n}{2\beta}} \cdot \lambda$$

**Decoder:**

receives  $m_1$  and  $m_{-1}$  from the Encoder.

$$u_{m_1}^{recon} = u_{m_1}^{recon} + \frac{1}{\lambda} \cdot \log \frac{n}{2\beta}$$

$$u_{m_{-1}}^{recon} = u_{m_{-1}}^{recon} - \frac{1}{\lambda} \cdot \log \frac{n}{2\beta}$$

$$\lambda \leftarrow \frac{n}{n-2 \log \frac{n}{2\beta}} \cdot \lambda$$

**end for**

$$w_1^{recon}, \dots, w_n^{recon} \leftarrow (\text{denormalize } u_1^{recon}, \dots, u_n^{recon}).$$

**ParamEst** $((u_1, \dots, u_n))$  :

$$1/\lambda \leftarrow \text{mean of } (|u_1|, \dots, |u_n|)$$

**return**  $\lambda$ 


---

rate-distortion function for exponential source (magnitude of normalized weights). We consider i.i.d. exponential source sequence  $u_1, \dots, u_n$  with distribution  $f_{exp}(u; \lambda) = \lambda e^{-\lambda u}$  for  $u \geq 0$ , reconstruction  $v_1, \dots, v_n$ , and one-sided  $\ell_1$  distortion given by:

$$d(u, v) = \begin{cases} u - v, & \text{if } u \geq v \\ \infty, & \text{otherwise.} \end{cases}$$

Then, the rate-distortion function is given in Lemma 3:

**Lemma 3.** [94] *The rate-distortion function for an exponential source with one-sided distortion is given by*

$$R(D) = \begin{cases} -\log(\lambda D), & 0 \leq D \leq \frac{1}{\lambda} \\ 0, & D > \frac{1}{\lambda} \end{cases} \quad (23)$$

---

**Algorithm 2** SuRP-modified

---

**Hyperparameters:**  $\beta$ 
**Inputs:** weights  $w_1, \dots, w_n$  in  $d$  layers

**Output:** reconstructed weights  $w_1^{recon}, \dots, w_n^{recon}$ 
**Normalization:**
**for**  $l = 1, \dots, d$  **do**

$$u^{(l)} \leftarrow \frac{|w^{(l)}|}{\|w^{(l)}\|_1}$$

**end for**

$$(u_1^{recon}, \dots, u_n^{recon}) \leftarrow 0$$

$$\lambda \leftarrow \text{ParamEst}((u_1, \dots, u_n))$$

Encoder sends  $\lambda$  to the Decoder.

**for**  $t = 1, \dots, L$  **do**
**Encoder:**
 $m_{inds} \leftarrow (\text{indices of the components in } (u_1, \dots, u_n) \text{ that are larger than } \frac{1}{\lambda} \cdot \log \frac{n}{\beta}.)$ 
**if**  $m_{inds}$  is empty **then**

$$\lambda \leftarrow \text{ParamEst}((u_1, \dots, u_n))$$

sends  $\lambda$  to the Decoder.

**end if**
 $m \leftarrow (\text{a random index from } m_{inds})$ 

sends  $m$  to the Decoder.

$$u_m = u_m - \frac{1}{\lambda} \cdot \log \frac{n}{\beta}$$

$$\lambda \leftarrow \frac{n}{n - \log \frac{n}{\beta}} \cdot \lambda$$

**Decoder:**

receives  $m$  from the Encoder.

$$u_m^{recon} = u_m + \frac{1}{\lambda} \cdot \log \frac{n}{\beta}$$

$$\lambda \leftarrow \frac{n}{n - \log \frac{n}{\beta}} \cdot \lambda$$

**end for**

$$w_1^{recon}, \dots, w_n^{recon} \leftarrow (\text{denormalize } u_1^{recon}, \dots, u_n^{recon} \text{ and add sign bits.})$$

**ParamEst** $((u_1, \dots, u_n))$  :

$$1/\lambda \leftarrow \text{mean of } (u_1, \dots, u_n)$$

**return**  $\lambda$ 


---

with the following optimal conditional probability distribution that achieves the minimum mutual information

$$f_{\mathbf{U}|\mathbf{V}}(u|v) = \begin{cases} \frac{1}{D} e^{-(u-v)/D}, & u \geq v \geq 0 \\ 0, & \text{otherwise.} \end{cases} \quad (24)$$

Moreover, the marginal distribution of  $\mathbf{V}$  is as follows

$$f_{\mathbf{V}}(v) = \lambda D \cdot \delta(v) + (1 - \lambda D) \cdot \lambda e^{-\lambda v} \quad (25)$$

where  $\delta(v)$  is a Dirac measure at 0.

Proof of Lemma 3 can be found in [94]. It is clear to see from Eq.s 24 and 25 that exponential source has the same nice properties as Laplacian:

1. It suggests pruning as an essential step in a good compression algorithm since Eq. 25 is a sparse distribution.
2. It is successively refinable, allowing for a both practical and rate-distortion theoretic optimal algorithm (see Algorithm 2).

Following the same steps in Section 5, it can be proven that Algorithm 2, which we used in our experiments, is zero-rate optimal with  $\beta = \log n$ .

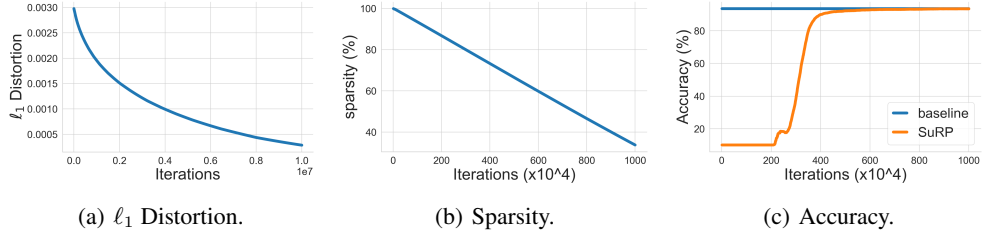


Figure 4: (a) Average  $\ell_1$  distortion, (b) sparsity and (c) accuracy of the reconstructed VGG-16 when SuRP is applied once (no iterative pruning). Baseline: fully-trained model without compression.

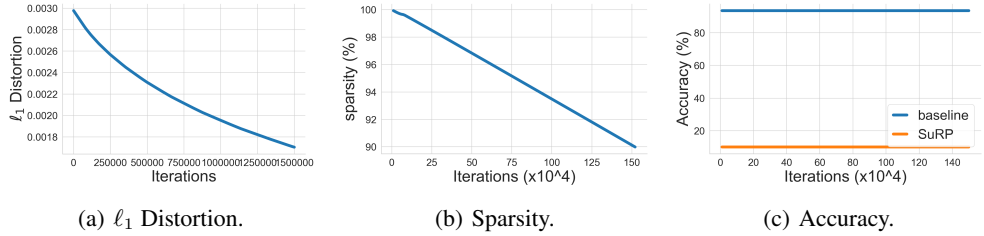


Figure 5: (a) Average  $\ell_1$  distortion, (b) sparsity and (c) accuracy of the reconstructed VGG-16 during SuRP (first iteration of the iterative pruning). SuRP stops at the desired sparsity 90%. Baseline: fully-trained model without compression.

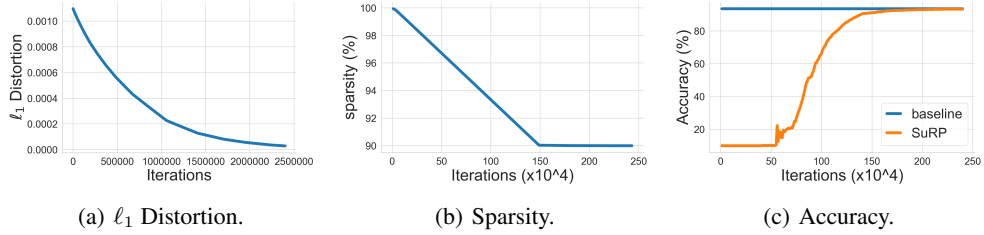


Figure 6: (a) Average  $\ell_1$  distortion, (b) sparsity and (c) accuracy of the reconstructed VGG-16 during SuRP (after the first iteration of the iterative pruning). The sparsity cannot be lower than 90% and SuRP must stop at the desired sparsity (which is higher than 90%). Baseline: fully-trained model without compression.

## E Visualization of SuRP

Figure 4 shows the decreasing  $\ell_1$  distortion and sparsity, and increasing accuracy of the reconstructed model through the iterations (running inside SuRP). We note that SuRP is applied only once in Figure 4 and iterations correspond to the iterations running inside SuRP. However, as stated in Section 6, we adopted iterative pruning approach, where each pruning iteration corresponds to running SuRP one time. After each pruning iteration, SuRP outputs a sparse model, and a retraining procedure is applied to the sparse model. When we do iterative pruning, we apply SuRP several times by increasing the target sparsity ratio every time. For instance, let us say we want to prune 90% of the parameters in the first pruning iteration. Then, as shown in Figure 5, SuRP stops once the sparsity ratio drops to 90%. Before starting the next iteration (next round of SuRP), we retrain the sparse model by excluding the pruned parameters (as proposed in [36]). In the next iteration, as shown in Figure 6, the sparsity can never be lower than 90% no matter how long we run the algorithm since 90% of the parameters are already pruned in the previous iteration of the pruning. As we typically desire a higher sparsity ratio in the later iterations, we need to stop SuRP at the target sparsity (which is higher than 90%).

## F Optimizing the Bit Rate

In this section, we highlight a useful byproduct of SuRP as a way to minimize the bit rate of the pruned model. Recall that SuRP requires transmitting two indices  $i, j \in \{1, \dots, n\}$  from the encoder to the decoder for each iteration. This means that SuRP automatically gives the integer (indices are integers from  $1, \dots, n$ ) representation of the model. Therefore, without dealing with floating points, i.e., precise values of the weights, we can reconstruct the model back using these indices. In order to further optimize this, we need a lossless compression scheme, namely entropy coding, to represent these indices as binary sequences. In information theory, the optimal entropy coding method can be found when the source distribution is known in advance [42]. Although there are universal codes that encode any source regardless of the distribution, they are preferable only when the source distribution is unknown since an entropy coding that matches the source distribution is always better than a universal code. Fortunately, our coding scheme for Laplacian (also for exponential) source induces a well-defined distribution that allows us to choose an optimal entropy coding method. Notice that randomly picking two indices  $i, j$  from  $\{k : \mathbf{U}_k^{(t)} \geq \frac{1}{\lambda_t} \cdot \log \frac{n}{2\beta}\}$  and  $\{k : \mathbf{U}_k^{(t)} \leq -\frac{1}{\lambda_t} \cdot \log \frac{n}{2\beta}\}$  is equivalent to: (1) first randomly permuting  $\mathbf{U}^{(t)}$ , and (2) selecting the minimum indices  $i, j$  from  $\{k : \mathbf{U}_k^{(t)} \geq \frac{1}{\lambda_t} \cdot \log \frac{n}{2\beta}\}$  and  $\{k : \mathbf{U}_k^{(t)} \leq -\frac{1}{\lambda_t} \cdot \log \frac{n}{2\beta}\}$ . The second approach induces a geometric distribution under the i.i.d. assumption on the indices where small indices are always more probable to be selected. For geometric sources, there are two standard entropy coding methods: unary coding and Golomb coding [31, 29]. In our additional experiments in Appendix I, for comparing SuRP with other works on accuracy-bit rate tradeoff, we use Golomb coding. Now, we give more details on both methods.

**Unary Coding.** Unary coding is a prefix-free code that is optimally efficient for the following geometric distribution:

$$P_B(b) = 2^{-b} \quad (26)$$

where  $b$  is a positive integer. In the simplest term, unary coding encodes an integer  $b$  with single 1 followed by  $b - 1$  consecutive 0's. For instance, 72 would be uniquely encoded as 100000010. In our problem, indices follow the distribution in Eq. 26 only when the fraction of normalized weights larger than  $1/\lambda_t \cdot \log \frac{n}{2\beta}$  in magnitude is exactly equal to 1/2. Since this is not the case in every iteration, unary coding is not the optimal entropy coding method for indices in SuRP.

**Golomb Coding.** Golomb coding is an optimal prefix-free code for any geometric source, i.e., it is more general than unary coding. The construction of Golomb codes can be found in [31]. In our additional experiments in Appendix I, we implemented Golomb coding to represent NN models as binary arrays.

## G Compression for Federated Learning

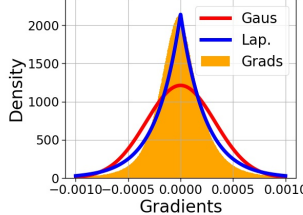


Figure 7: Density of gradients of ResNet-50 trained on ImageNet. We present only the gradients from the late stages of training since we use a pretrained ResNet-50.

In Section 6, we have applied SuRP to compress gradients in federated learning. In Figures 7, 8, and 9, we justify that Laplacian is a good fit for gradients of ResNet-50 trained on ImageNet, ResNet-18 trained on CIFAR-10, and VGG-16 trained on CIFAR-10. Since we need to compress the gradients before each communication round of federated training, SuRP requires the gradients to follow a Laplacian distribution throughout the learning process. In other words, although the

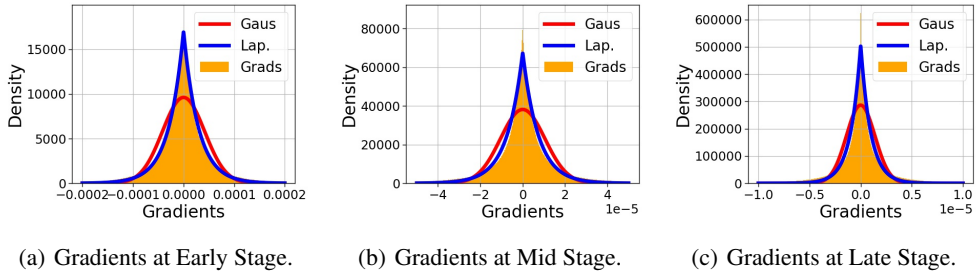


Figure 8: Density of gradients of ResNet-18 trained on CIFAR-10 during (a) early stages of training (epoch 32), (b) middle stages of training (epoch 155), (c) late stages of training (epoch 336).

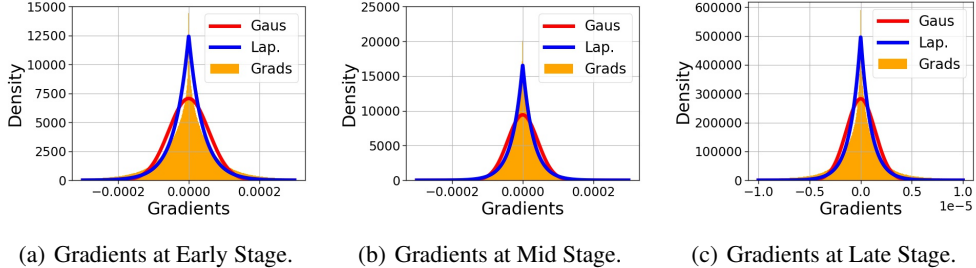


Figure 9: Density of gradients of small VGG-16 trained on CIFAR-10 during (a) early stages of training (epoch 16), (b) middle stages of training (epoch 100), (c) late stages of training (epoch 170).

parameter of the Laplacian distribution might change, we must be able to fit a Laplacian distribution to the gradients in every round. We provide the density estimation of gradients in early-, mid-, and late-stages of training in Figures 7, 8, and 9 to show that Laplacian distribution is a good fit for gradients starting from the early stages of training till the training ends. Therefore, we can apply SuRP to compress gradients at every communication round. In our experiments, we update the parameter of the Laplacian distribution ( $\lambda$ ) at every communication round.

Among other gradient sparsification methods for federated learning [1, 63, 69, 95, 99], SuRP is most similar to rTop- $k$  [4], in that they also communicate a random subset of the large gradients. Different from our work, they approach the communication-efficient federated learning problem from a distributed statistical estimation point of view. By modeling the gradients with a sparse Bernoulli distribution, they show that the optimal compression strategy for each user (device) is to communicate a random  $k/r$  fraction of the  $r$  largest gradients. In contrast, we study the gradient compression problem from an information-theoretic approach and assume Laplacian distribution over the gradients. With this assumption, we conclude that each user must communicate the parameter of underlying Laplacian distribution of the local gradients and a list of indices that are randomly selected among the gradients larger than  $\frac{1}{\lambda_t} \cdot \log \frac{n}{2\beta}$  in magnitude at iteration  $t$ . Since the threshold  $\frac{1}{\lambda_t} \cdot \log \frac{n}{2\beta}$  is decreasing at each iteration, SuRP assigns a higher probability for larger (in magnitude) gradients to be selected, whereas rTop- $k$  picks the gradients uniformly random from the large gradients.

## H Additional Experimental Details

We conducted our experiments on NVIDIA Titan X (MNIST and CIFAR-10) and NVIDIA Titan Xp (ImageNet) GPUs on an internal cluster server. We used 1 GPU for MNIST and CIFAR-10 experiments and 2 GPUs for ImageNet experiments. We set the target sparsity of each SuRP round so that at each pruning iteration, 20% of the surviving parameters will be pruned, e.g., sparsity schedule is as follows 20%, 36%, 48.8%, 59.04%, ... .

### H.1 MNIST:

We provide the architectural details and hyperparameters for LeNet-5 Caffe in Table 2 [55]. We use a batch size of 100 and train for 100 epochs, early stopping at the best accuracy on validation set. We use the Adam optimizer with learning rate = 0.001, and  $\beta_1 = 0.9, \beta_2 = 0.999$  with weight decay =  $5e^{-4}$ .

Name	Component
conv1	[ $5 \times 5$ conv, 20 filters, stride 1], ReLU, $2 \times 2$ max pool
conv2	[ $5 \times 5$ conv, 50 filters, stride 1], ReLU, $2 \times 2$ max pool
Linear	Linear $800 \rightarrow 500$ , ReLU
Output Layer	Linear $500 \rightarrow 10$

Table 2: LeNet-5 Caffe convolutional architecture.

### H.2 CIFAR-10:

We provide the architectural details and hyperparameters for the ResNet-20 [39] and (small) VGG-16 [88] in Tables 3 and 4, respectively. For both ResNet-20 and VGG-16, we use a batch size of 128, we train ResNet-20 for 350 epochs and VGG-16 for 200 epochs, early stopping at the best accuracy on validation set. We use SGD with learning rate = 0.1, momentum = 0.9, and weight decay =  $5e^{-4}$ . We note that VGG-16 architecture is a smaller version of the original VGG architecture in [88]. We retrain both models for 20 epochs at the end of each pruning iteration.

Name	Component
conv1	$3 \times 3$ conv, 16 filters, stride 1, BatchNorm
Residual Block 1	$3 \times 3$ conv, 16 filters
	$3 \times 3$ conv, 16 filters
Residual Block 2	$3 \times 3$ conv, 32 filters
	$3 \times 3$ conv, 32 filters
Residual Block 3	$3 \times 3$ conv, 64 filters
	$3 \times 3$ conv, 64 filters
Output Layer	$7 \times 7$ average pool stride 1, fully-connected, softmax

Table 3: Slim ResNet-20 architecture.

Name	Component
conv1-2	[ $3 \times 3$ conv, 64 filters, stride 1, BatchNorm, ReLU] $\times 2$
max pool	$2 \times 2$ , stride 2
conv3-4	[ $3 \times 3$ conv, 128 filters, stride 1, BatchNorm, ReLU] $\times 2$
max pool	$2 \times 2$ , stride 2
conv5-7	[ $3 \times 3$ conv, 256 filters, stride 1, BatchNorm, ReLU] $\times 3$
max pool	$2 \times 2$ , stride 2
conv8-10	[ $3 \times 3$ conv, 512 filters, stride 1, BatchNorm, ReLU] $\times 3$
max pool	$2 \times 2$ , stride 2
conv11-13	[ $3 \times 3$ conv, 512 filters, stride 1, BatchNorm, ReLU] $\times 3$
max pool	$2 \times 2$ , stride 2
Output Layer	$1 \times 1$ average pool stride 1, fully-connected, softmax

Table 4: VGG-16 architecture.

### H.3 ImageNet:

We provide the architectural details and hyperparameters for the ResNet-50 used in our experiments in Table 5. We use the pretrained ResNet-50 from PyTorch (<https://github.com/pytorch/vision/blob/master/torchvision/models/resnet.py>), with a batch size of 64. At the end of each pruning iteration, we retrain the model for 15 epochs. We use SGD with learning rate = 0.001, momentum = 0.9 and weight decay =  $5e^{-4}$ .

Name	Component
conv1	$3 \times 3$ conv, 64 filters, stride 1, BatchNorm
Residual Block 1	$\begin{bmatrix} 1 \times 1 \text{ conv, 64 filters} \\ 3 \times 3 \text{ conv, 64 filters} \\ 1 \times 1 \text{ conv, 256 filters} \end{bmatrix} \times 3$
Residual Block 2	$\begin{bmatrix} 1 \times 1 \text{ conv, 128 filters} \\ 3 \times 3 \text{ conv, 128 filters} \\ 1 \times 1 \text{ conv, 512 filters} \end{bmatrix} \times 4$
Residual Block 3	$\begin{bmatrix} 1 \times 1 \text{ conv, 256 filters} \\ 3 \times 3 \text{ conv, 256 filters} \\ 1 \times 1 \text{ conv, 1024 filters} \end{bmatrix} \times 6$
Residual Block 4	$\begin{bmatrix} 1 \times 1 \text{ conv, 512 filters} \\ 3 \times 3 \text{ conv, 512 filters} \\ 1 \times 1 \text{ conv, 2048 filters} \end{bmatrix} \times 3$
Output Layer	$4 \times 4$ average pool stride 1, fully-connected, softmax

Table 5: ResNet-50 architecture.

## I Additional Experimental Results

We give a more detailed version of Table 1 in Tables 6 and 7 and a more detailed version of Figure 2-left in Table 8 with confidence intervals included in SuRP results. Additionally, we provide accuracy-bit rate comparisons between SuRP and relevant baselines such as Deep Comp. [36], DeepCABAC [100], DNS [34], and SWS [92] in Table 9. It is seen from Table 9 that SuRP outperforms the baselines both in terms of accuracy-sparsity and accuracy-bit rate tradeoffs.

Pruning Ratio:	93.12%	95.60%	97.19%	98.20%	98.85%	99.26%	99.53%	99.70%	99.81%	99.88%
Global [73]	91.30	90.80	89.28	85.55	81.56	54.58	41.91	31.93	21.87	11.72
Uniform [109]	91.47	90.78	88.61	84.17	55.68	38.51	26.41	16.75	11.58	9.95
Adaptive [27]	91.54	91.20	90.16	89.44	87.85	86.53	84.84	82.41	74.54	24.46
RiGL [22]	92.34	91.99	91.66	91.15	90.55	89.51	88.21	86.73	84.85	81.50
LAMP [58]	92.24	92.06	91.71	91.66	91.07	90.49	89.64	88.75	87.07	84.90
SuRP (ours)	<b>92.55 <math>\pm</math> 0.19</b>	<b>92.13 <math>\pm</math> 0.20</b>	<b>91.95 <math>\pm</math> 0.21</b>	<b>91.72 <math>\pm</math> 0.28</b>	<b>91.21 <math>\pm</math> 0.24</b>	<b>90.73 <math>\pm</math> 0.21</b>	<b>90.65 <math>\pm</math> 0.27</b>	<b>89.70 <math>\pm</math> 0.32</b>	<b>87.28 <math>\pm</math> 0.32</b>	<b>85.04 <math>\pm</math> 0.35</b>

Table 6: Accuracy of VGG-16 on CIFAR-10. Results are averaged over five runs.

Pruning Ratio:	79.03%	86.58%	91.41%	94.50%	96.48%	97.75%	98.56%	99.08%	99.41%	99.62%
Global [73]	87.48	86.97	86.29	85.02	83.15	80.52	76.28	70.69	47.47	12.02
Uniform [109]	87.24	86.70	86.09	84.53	82.05	77.19	64.24	47.97	20.45	13.35
Adaptive [27]	87.30	87.00	86.27	85.00	83.23	80.40	76.40	69.31	52.06	20.19
RiGL [22]	87.63	87.49	86.83	85.84	84.08	81.76	78.70	74.40	66.42	50.90
LAMP [58]	87.54	87.12	86.56	85.64	84.18	81.56	78.63	74.20	67.01	51.24
SuRP (ours)	<b>91.37 <math>\pm</math> 0.24</b>	<b>90.44 <math>\pm</math> 0.26</b>	<b>89.00 <math>\pm</math> 0.21</b>	<b>88.87 <math>\pm</math> 0.26</b>	<b>87.05 <math>\pm</math> 0.28</b>	<b>83.98 <math>\pm</math> 0.20</b>	<b>79.00 <math>\pm</math> 0.34</b>	<b>74.86 <math>\pm</math> 0.29</b>	<b>70.64 <math>\pm</math> 0.38</b>	<b>54.22 <math>\pm</math> 0.42</b>

Table 7: Accuracy of ResNet-20 on CIFAR-10. Results are averaged over five runs.

Pruning Ratio:	80%	90%
Adaptive [27]	75.60	73.90
SNIP [59]	72.00	67.20
DSR [74]	73.30	71.60
SNFS [18]	74.90	72.90
RiGL [22]	74.60	72.00
SuRP (ours)	<b>75.54 <math>\pm</math> 0.05</b>	<b>73.93 <math>\pm</math> 0.04</b>

Table 8: Accuracy of ResNet-50 on ImageNet. Results are averaged over three runs.

Model (Original size)	Original Acc. (%)	Method	Sparsity $\frac{ w=0 }{ w } (\%)$	Comp. Size	Comp. Acc. (%)
LeNet-5-Caffe MNIST (1.72 MB)	99.14	Deep Comp. [36]	92.0	44 KB ( $\times 39$ )	99.3
		DNS [34]	99.1	16 KB ( $\times 107$ )	99.1
		SWS [92]	99.5	11 KB ( $\times 156$ )	99.0
		DeepCABAC [100]	98.1	12 KB ( $\times 143$ )	99.1
		SuRP (ours)	99.2	<b>7 KB</b> ( $\times 246$ )	99.3 ( $\pm 0.0$ )
		SuRP (ours)	99.3	<b>5 KB</b> ( $\times 344$ )	98.2 ( $\pm 0.1$ )
ResNet-18	95.60	SuRP (ours)	90.0	3.1 MB ( $\times 15$ )	95.1 ( $\pm 0.0$ )
CIFAR-10 (44.70 MB)		SuRP (ours)	95.0	1.1 MB ( $\times 42$ )	92.2 ( $\pm 0.1$ )
		SuRP (ours)	97.0	<b>875 KB</b> ( $\times 53$ )	90.0 ( $\pm 0.2$ )
Small VGG-16	93.60	DeepCABAC [100]	92.4	956 KB ( $\times 61$ )	91.0
CIFAR-10 (58.91 MB)		SuRP (ours)	95.0	<b>1.1 MB</b> ( $\times 54$ )	92.4 ( $\pm 0.1$ )
		SuRP (ours)	90.0	3.0 MB ( $\times 20$ )	93.5 ( $\pm 0.1$ )
ResNet-50	76.60	Deep Comp. [36]	71.0	6.1 MB ( $\times 16$ )	76.1
ImageNet (102.23 MB)		DeepCABAC [100]	74.6	6.1 MB ( $\times 16$ )	74.1
		SuRP (ours)	71.0	<b>6.1 MB</b> ( $\times 16$ )	76.4 ( $\pm 0.0$ )

Table 9: Comparison of SuRP with other pruning strategies in terms of accuracy, sparsity and size (bit rate).